Fermilab

J. MacLachlan, AD/PS

Someday ?? February 06

Prospective Gains from γ_T Jump & 2^{nd} Harmonic Magnet Ramp

- Introduction
- Scope of study
- Longitudinal coupling impedance
- Ramp details
- RF voltage curves
- γ_T jump
- Results
- Conclusions & remarks

Introduction

The proposal to reduce the peak rf voltage required in the acceleration of protons to 8 GeV in the Booster by adding a second harmonic component to the 15 Hz ramp cycle has been discussed at several different times over many (perhaps 20 – 30) years. Only recently have power capacitors achieved adequate stored energy density to permit including the additional components on the existing magnet support girders. However, it is still an expensive and laborious upgrade. Although rather different in concept, both the second harmonic ramp and an operational γ_T jump have apparent potential to help increase available intensity from the Booster. Some modeling has been carried out to explore the benefits seperately and in combination. The Booster parameters used for longitudinal phase space tracking are collected in Table 1 below.

Prospectively the question of relative merit is reasonable in view of the desire to keep the jump less than one unit in γ_T to limit the disruption of the beam envelope functions β_x and β_y. It is shown that a 0.3 unit jump is more likely to help in increasing Booster intensity than a ramp with any admixture of second hamonic.

Table 1 Parameters

Table 1 Booster and injected beam parameters used for tracking

Parameter	Symbol	Value	Units
circumference	C	474.19	m
sinusoidal magnet ramp		15	Hz
modified magnet ramps		15 + 30	Hz
injection kinetic energy	$W_{\circ,i}$	400.00	MeV
linac beam energy spread FW	ΔE	1.00	MeV
final kinetic energy	$W_{\circ,f}$	8000.	MeV
transition energy/$m_\circ c^2$	γ_T	5.4460	
rf peak voltage	V_{rf}	900.00	kV
rf harmonic	h	84	
circulation frequency at injection	$f_\circ$	450.81	kHz
number of protons per bunch	N	$5 \cdot 10^{10}$ & $8 \cdot 10^{10}$	
average beam current at injection	$\bar{I}$	320 & 513	mA
longitudinal coupling impedance	$Z_{\|\|}(\omega)$	from J. Crisp	
nonadiabatic time (15 Hz ramp)	t_c	0.257	ms
nonlinear time (15 Hz ramp)	t_{nl}	0.037	ms

Scope of Study

The beam loss and final longitudinal emittance are evaluated by longitudinal phase space tracking for $5 \cdot 10^{10}$ and $8 \cdot 10^{10}$ protons per bunch over the complete acceleration cycle. Three magnet cycles are examined and the effect of a 0.3 unit γ_T jump is tested for each intensity on each ramp. The magnet cycles used are the existing 15 Hz sinusoidal ramp, a 15 Hz ramp with a second harmonic component adjusted in phase and amplitude to minimize the maximum $\dot{B}$, and a compromise ramp with a 30 Hz component adjusted to reduce maximum $\dot{B}$ while limiting $\ddot{B}$ at injection to somewhat less than its value on the standard 15 Hz ramp. Not all of the Booster's problems in high intensity operation arise from longitudinal dynamics, but longitudinal phase space calculations can illustrate effects from changes in ramp slope or speed of transition crossing. The twelve cases are as simillar as possible to be useful in comparing the benefits of a second harmonic component in the ramp and a γ_T jump seperately or in combination. The individual cases are not optimized by adjusting the rf voltage curve for each one.

Ramp Details

The present 15 Hz sinusoidal ramp and two containing a 15 Hz fundamental plus 12.5 % additional second harmonic are plotted in Fig. 1. One of the two component ramps has the second harmonic shifted 90° to give the lowest maximum $\dot{B}$; the other is a compromise having the second harmonic phased to keep $\ddot{B}$ at injection and maximum $\dot{B}$ below the values on the pure 15 Hz ramp. The 90° phasing gives the long-discussed minimum rf power second harmonic ramp. The modification in the third ramp responds to recent comment that the second harmonic could reduce capture efficiency at injection. The slopes and curvatures of the same three ramps are compared in Figs. 2 and 3.

Comparison of ramp curves

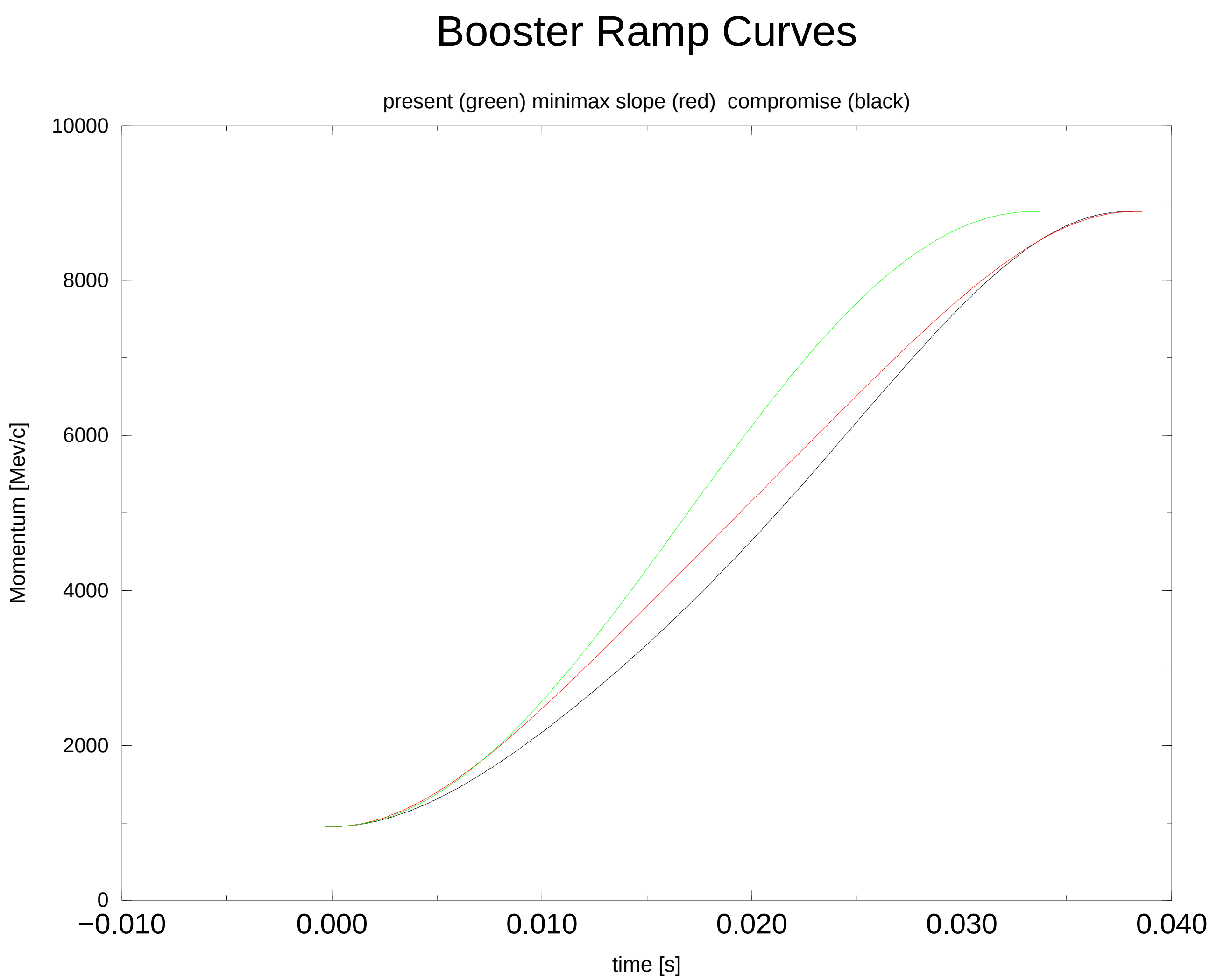

Figure 1: The three ramps [MeV/c] compared in the Booster modeling

Comparison of ramp slopes

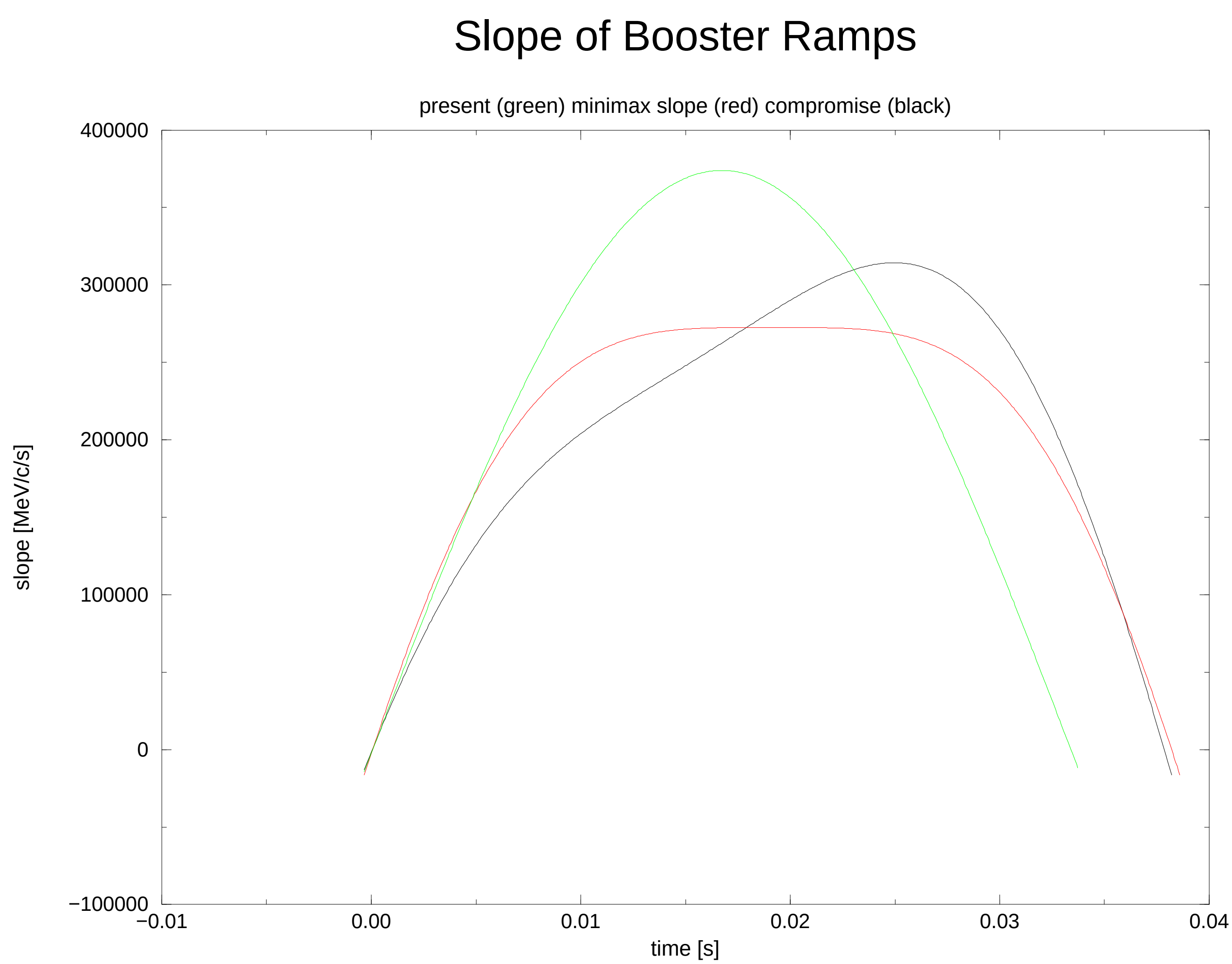

Figure 2: The slope [MeV/c/s] for the three ramps compared in the Booster modeling

Comparison of ramp curvature

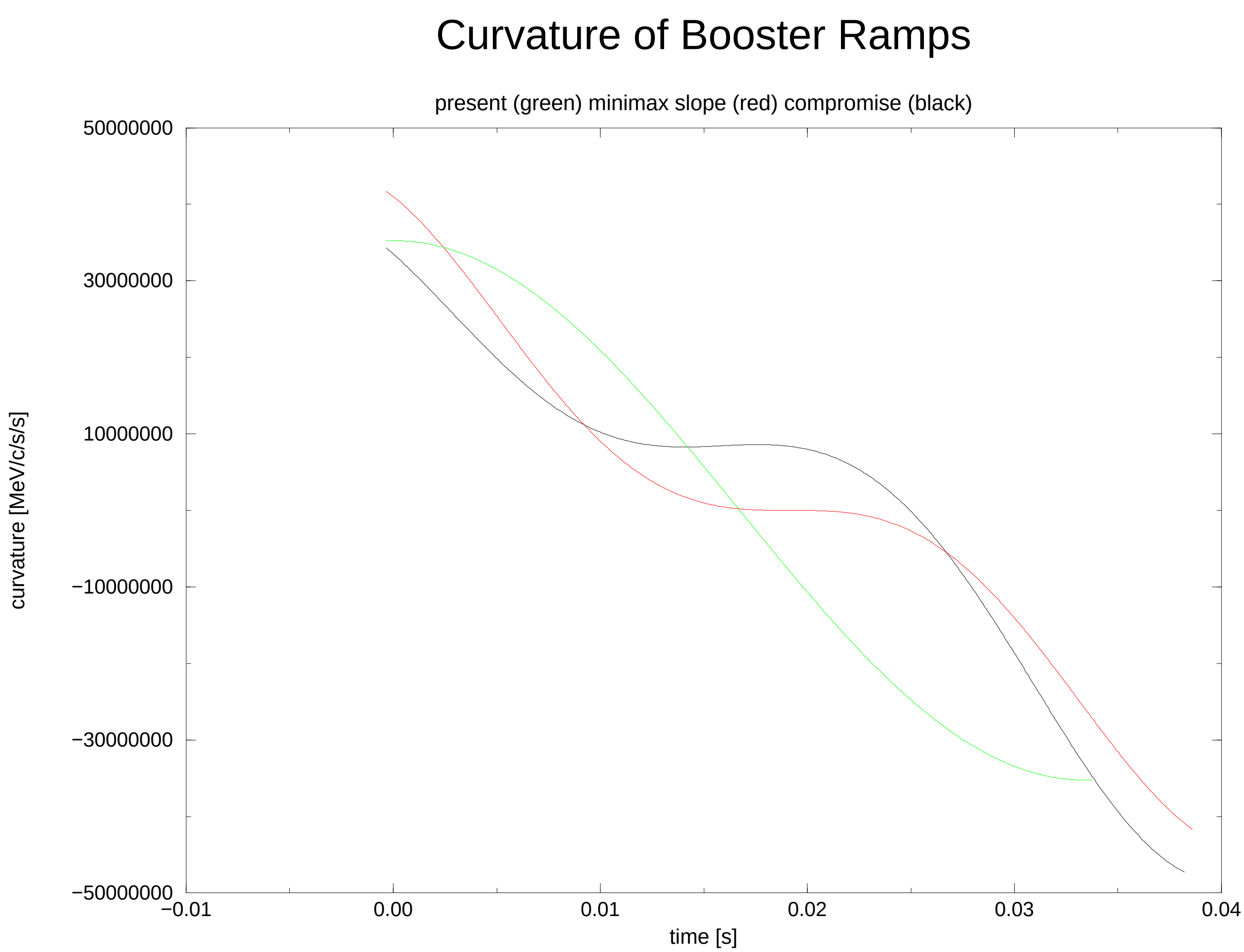

Figure 3: The curvature [MeV$c^{-1}s^{-2}$] for the three ramps compared in the Booster modeling

General Description of Ramp Curves

Any ramp between $B_\circ$ and B_f can be written

$$B = B_\circ + (B_f - B_\circ)F(\omega t)$$

where ω is 2π times the ramp repetition rate. $F(0) = 0$ and $F(\vartheta_{\mathsf{max}}) = 1$ where ϑ_{max} is the ϑ at the end of the ramp. If the time base has an arbitrary origin and the injection is assumed to be at $\dot{\mathrm{B}}$ = 0, F can always be written as

$$F(\vartheta) = \frac{f(\vartheta) - f(\vartheta_\circ)}{f(\vartheta_{\mathsf{max}}) - f(\vartheta_\circ)} \quad ,$$

where $\vartheta_\circ$ is the value of ϑ at which $\dot{\mathrm{B}}$ is zero. For the current single harmonic 15 Hz ramp,

$$f(\vartheta) = \frac{1 - \cos(\vartheta)}{2}$$

in which case F and f are the same function. However, if one is to add a second harmonic to limit $\dot{\mathrm{B}}$ and/or $\ddot{\mathrm{B}}$, f can be generalized as

$$f(\vartheta) = 1 - [\cos(\vartheta) + a\cos(2\vartheta + b)].$$

Now,

$$F' = \dot{F}/\omega = \frac{f'(\vartheta)}{f(\vartheta_{m\circ} + f'(\vartheta_{m\circ})\Delta\vartheta_m \cdots - f(\vartheta_{\circ\circ}) - f'(\vartheta_{\circ\circ})\Delta\vartheta_\circ \cdots} \;,$$

where the Δ's are changes in the $\dot{\mathrm{B}}$ = 0 locations arising from the second harmonic admixture. By definition

$$f'(\vartheta_{m\circ}) = f'(\vartheta_{\circ\circ}) \equiv 0 \;;$$

furthermore the Δ's at $\sim 0.1\pi$ are rather small. The normalization does not change to first order when the second harmonic is added in, and even though the second derivatives are $\sim 10^3$ the normalization change is not enough to complicate comparing f's directly to choose a nearly optimum phase and amplitude for the second harmonic. When the normalization for the 2-component F is larger than the original 2, the amount of first harmonic needed for the ramp is reduced because of the second harmonic. However, the changes in normalization are small, $\sim$ 3% in this work.

$\dot{\text{p}}$ on Minimax $\dot{\text{B}}$ Ramp from Model

The following slide shows the $\dot{\text{p}}$ calculated by the modeling program for the minimax $\dot{\text{B}}$ ramp. The low (and even negative) $\dot{\text{p}}$ during the first 400 μs of the cycle results from a choice to maintain the RF phase at zero during this time. The negative slope results from the phase shift caused by energy lost to the $\mathcal{R}e(Z_{||})$. Because the ramp is at a minimum at the nominal injection point, injecting about 300 μs or so early results in the momentum on the central orbit following the injected beam down by approximately 2.5 MeV/c (for $8 \cdot 10^{10}$ bunches) so that the beam remains on the central orbit. This small adjustment to the injection scheme keeps the capture bucket span at $\pm 180^{\circ}$ despite the non-zero $\dot{\text{B}}$ during the capture. Optimum capture requires that the linac energy be about 2.5 MeV above the E_{min} of the Booster.

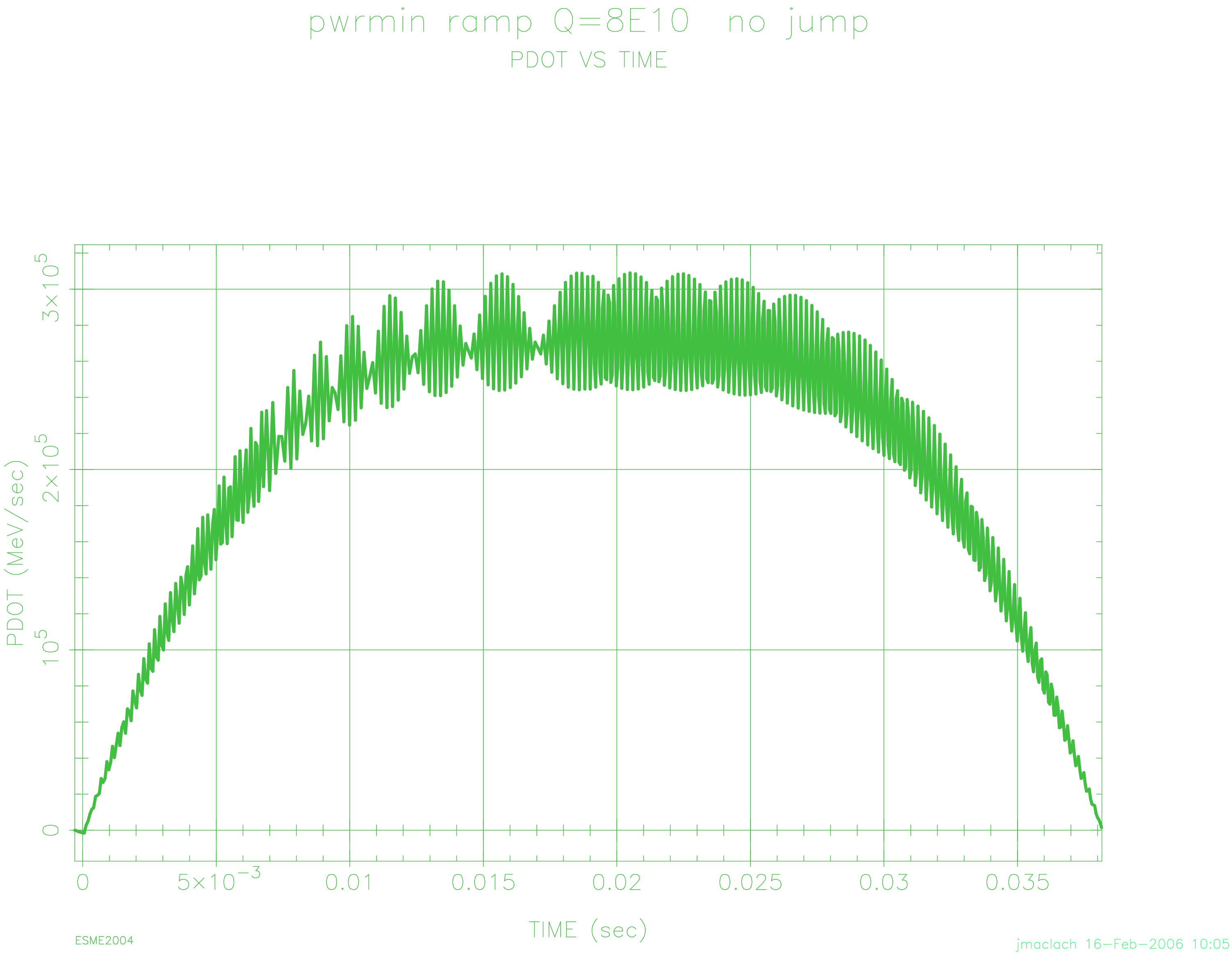

Figure 4: ṗ on the minimax Ḃ cycle, no jump. Fluctuation resulting from variation in φ_s from energy loss compensation is readily apparent. See text for comments on the nearly zero slope for 400 μs at start of ramp.

RF Voltage Curve

Two different rf amplitude curves were used, although it is argued in retrospect that the simpler one shown in the first slide following can (should) be used in all cases with little practical difference in the results. The curves were developed from three assumptions. First, it was assumed that the present capture scheme had been empirically optimized by long tuning effort. Second, a limit of 900 kV was taken as a practical maximum rf voltage amplitude. Finally, an effort was made to approximately maintain the bucket area near ten times the rms bunch emittance to keep losses under control.

Piecewise linear RF voltage curve

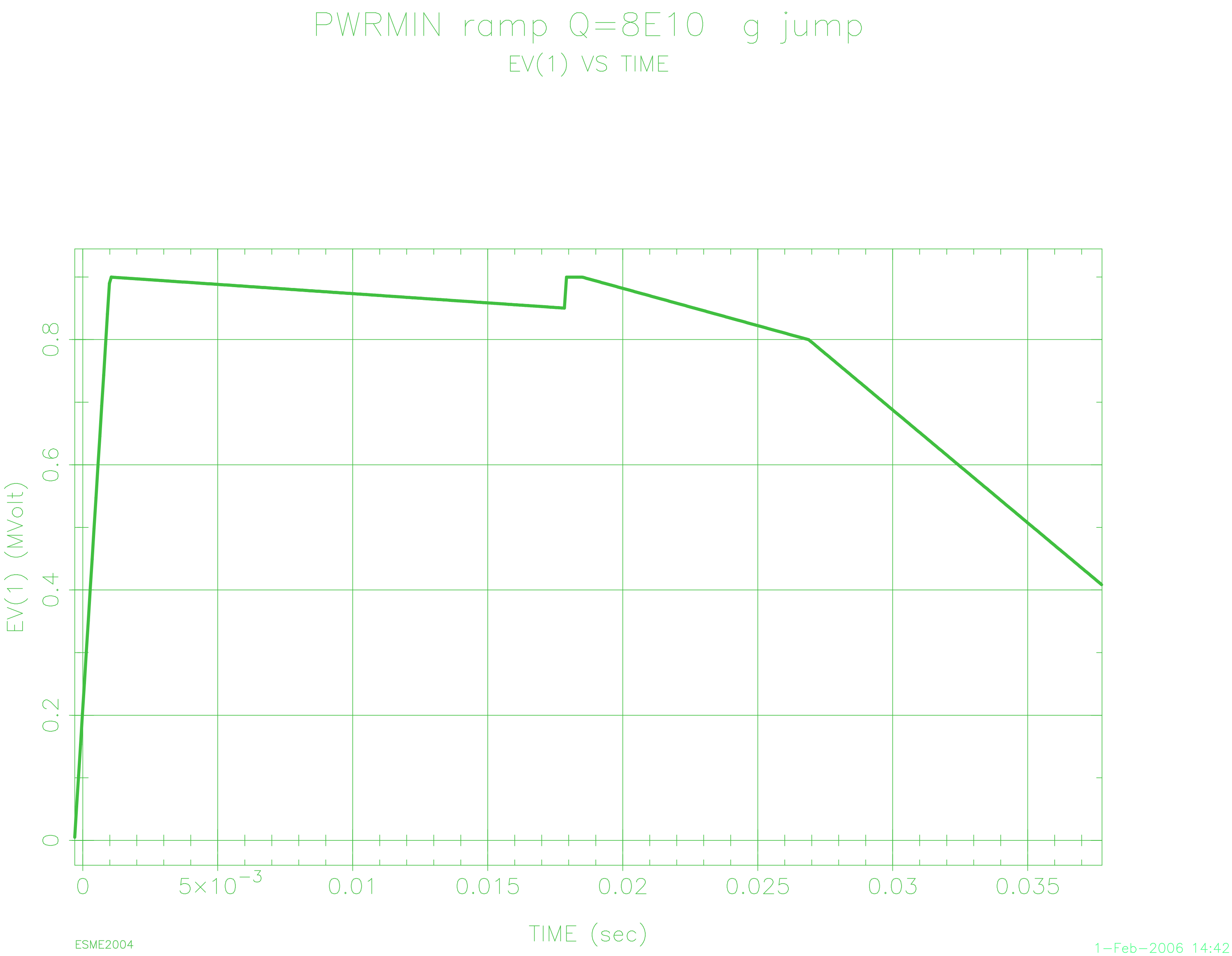

Figure 5: The rf voltage curve used in almost all of the model cases

RF voltage curve with constant bucket area after transition

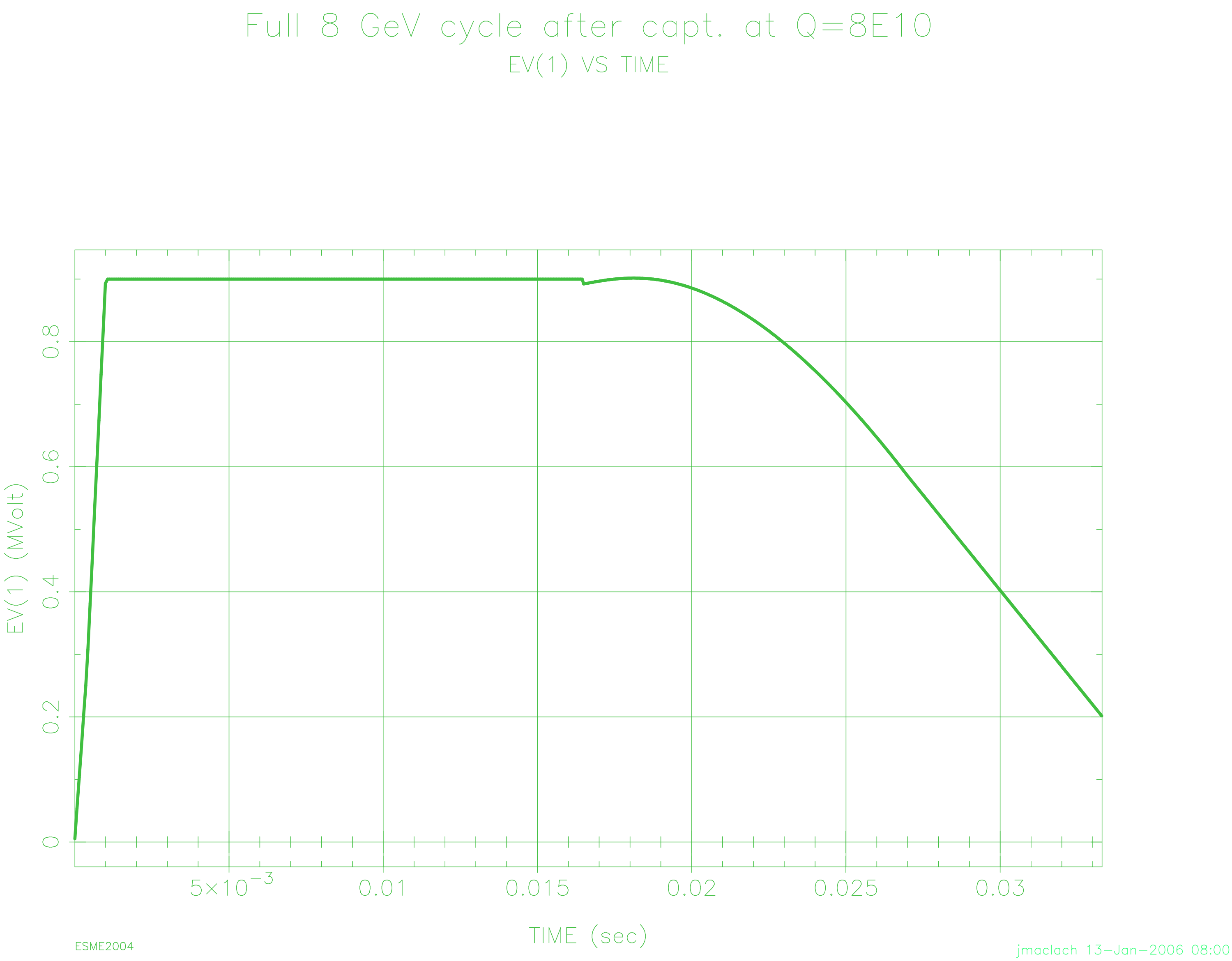

Figure 6: The voltage curve used in a few of the earliest model cases. The previous curve gives simillar results; it is appropriate to compare results regardless of the choice between the two.

γ_T Jump

When the γ_T jump was used, only the timing was changed to adjust to the ramp timing, but the amplitude was always taken as 0.3 units in γ_T. With this small jump it was found optimum to approach $\eta = 0$ closely and take the jump asymmetrically about $\eta = 0$. With such a small jump it is not possible to turn the jump on an adiabatic time interval early and have it result in $\eta > 0$. It has been typical to use jump amplitude ~ 1 unit, but fortunately for the Booster case as little as 0.3 units seem to suffice, "fortunate" because one unit in γ_T has been accompanied by intolerable closed orbit distortion (correctable in principle) and β function perturbation (probably inescapable). The cost in bunch shape distortion appears to be tolerable. The jump was modeled as having instantaneous turn-on and 1 ms time constant for exponential decay. The effect on the time slip parameter $\eta = \gamma_T^{-2} - \gamma^{-2}$ is shown in the following slide for the pure 15 Hz ramp.

η with γ_T jump on 15 Hz ramp

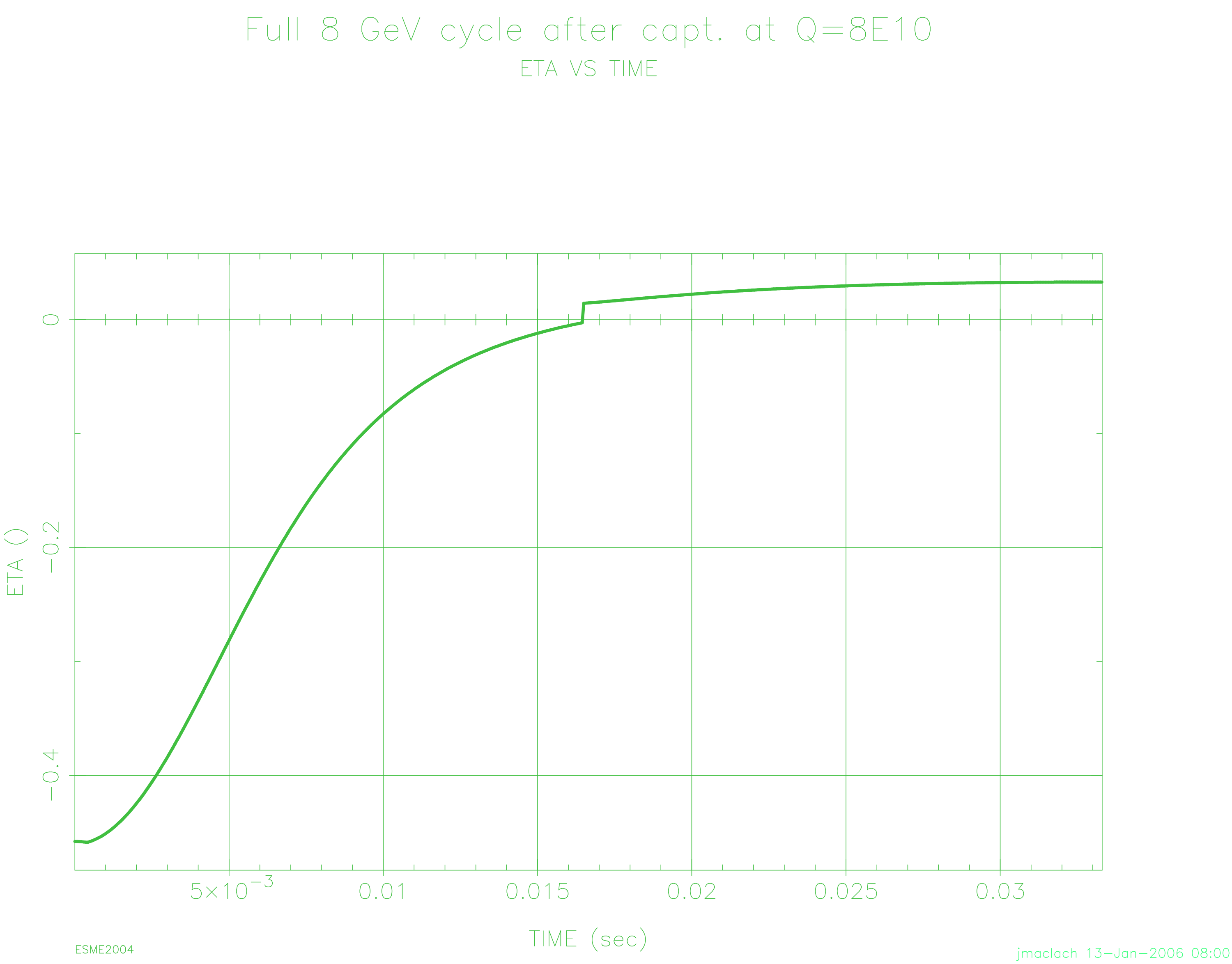

Figure 7: The time slip factor η on the standard 15 Hz ramp with a 0.3 unit γ_T jump

Longitudinal Coupling Impedance

The $\mathcal{R}\mathrm{e}\ Z_{||}(\omega)$ is unusually important in the Booster because the absence of a beam pipe causes substantial loss, especially at high frequency. It is the dominant parameter in the intensity limit for the Booster at transition because it does not drop with energy like the space charge and the bunches have large fourier components at high frequency from bunch narrowing. The bunch narrowing is unavoidable in any variant of normal transition crossing. The only tactic that has been succesful in a real γ_T lattice has been the γ_T jump. The next slide shows the values taken from Jim Crisp's wire measurements of the magnets continued to higher frequency above the frequencies the stretched wire technique could reach. Because it results in at least some spurious loss, the continuation was tested by cutting the real part to zero at the higher frequencies. There was little effect on results. The measured values seem higher than beam behavior suggests, but they are the *only* frequency dependent measurements; they are consistent with calculations of Ruggiero, Snowden, Shafer, and Gluckstern.

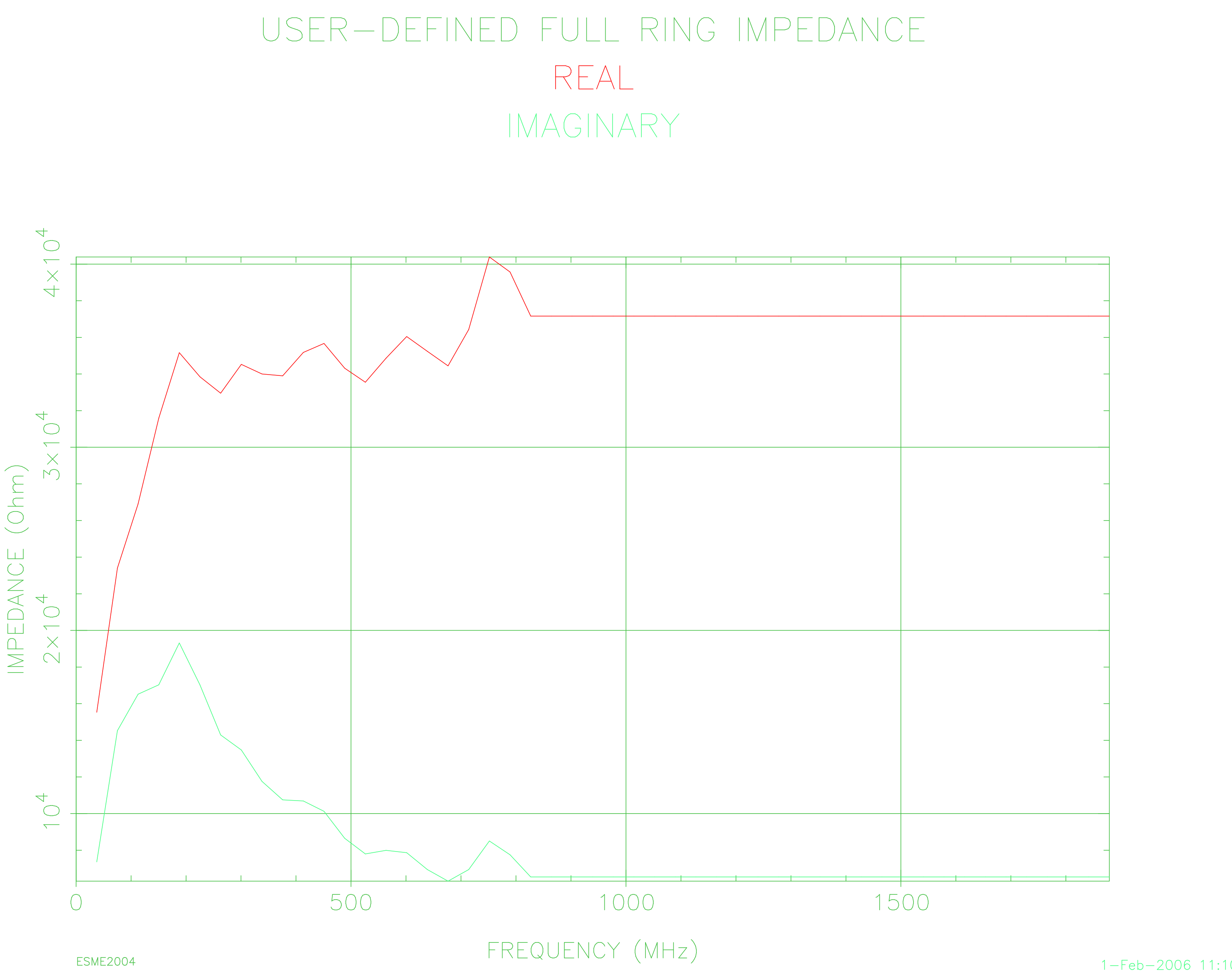

Figure 8: The longitudinal coupling impedance $Z_{||}(f)$. The real part is held constant above the frequencies measured by J. Crisp

Results

The programaticly important performance measures are the final longitudinal emittance and the beam power loss over the cycle. Table 2 below gives the final emittance and the charge loss for the several cases. The charge loss is separated into a pre-transition part (“injection”) and a post-transition part (“transition”). The beam power loss can be estimated from the results by using the injection energy with the injection loss and the transition energy with the transition loss rather than by integrating over the complete cycle. The average and peak RF power are very important operational considerations. These quantities have been limited by holding the peak RF voltage to 900 kV or below, but the power has not been evaluated for the cases run. The voltage curves plus the total cavity $R_{\mathtt{shunt}}$ are the necessary information to carry out the power calculation. Average power is probably the more immediate concern for system reliability, but this has not been explicit. Tuners and bias supplies may also be stressed by longer acceleration times. Because the capture and transition crossing parts of the cycle have rather simillar rf requirements for all of the higher intensity cases with these ramps, there is rather little gained by optimizing the rf voltage curve separately for each case. A detailed comparison of the numerical results may lead to questions interesting to the modeler about the degree of simillarity between starting conditions, but the first significant figure in the numerical results already answers the original questions uneqivocally. The conclusions are fortified by looking at the phase space plots for the high loss times in the cycle.

Table 2 Results

Table 2 Beam loss and final longitudinal emittance for the normal ramp and two examples of second harmonic ramp at $5 \cdot 10^{10}$ and $8 \cdot 10^{10}$ per bunch with and without a 0.3 unit γ_T jump

ramp type	bunch intensity	beam loss [10^{10}]		rms emittance [eVs]
no γ_T jump		injection	transition	
standard ramp	$5 \cdot 10^{10}$	0.674	20.795	0.0327
	$8 \cdot 10^{10}$	4.662	581.126	0.0991
minimax $\dot{B}$	$5 \cdot 10^{10}$	0.000	326.788	0.0895
	$8 \cdot 10^{10}$	0.016	594.537	0.0678
compromise ramp	$5 \cdot 10^{10}$	0.000	339.823	0.0516
	$8 \cdot 10^{10}$	0.180	599.182	0.0622
with γ_T jump				
standard ramp	$5 \cdot 10^{10}$	0.044	0.041	0.0141
	$8 \cdot 10^{10}$	4.682	2.911	0.0195
minimax $\dot{B}$	$5 \cdot 10^{10}$	0.000	0.000	0.0107
	$8 \cdot 10^{10}$	0.000	0.012	0.0147
compromise ramp	$5 \cdot 10^{10}$	0.028	0.000	0.0160
	$8 \cdot 10^{10}$	0.180	0.004	0.0140

Conclusion & Comments

The results presented support a conclusion that whichever ramp is chosen, a γ_T jump will be required to push intensity higher. Even in the lower per batch intensity envisioned for high intensity MI running with slipstacking, the limit on longitudinal emittance appears to require the jump. Because high intesity capture is satisfactory on all of the ramps, injection efficiency or initial $\ddot{p}$ are not principal concerns in choosing the ramp curve.

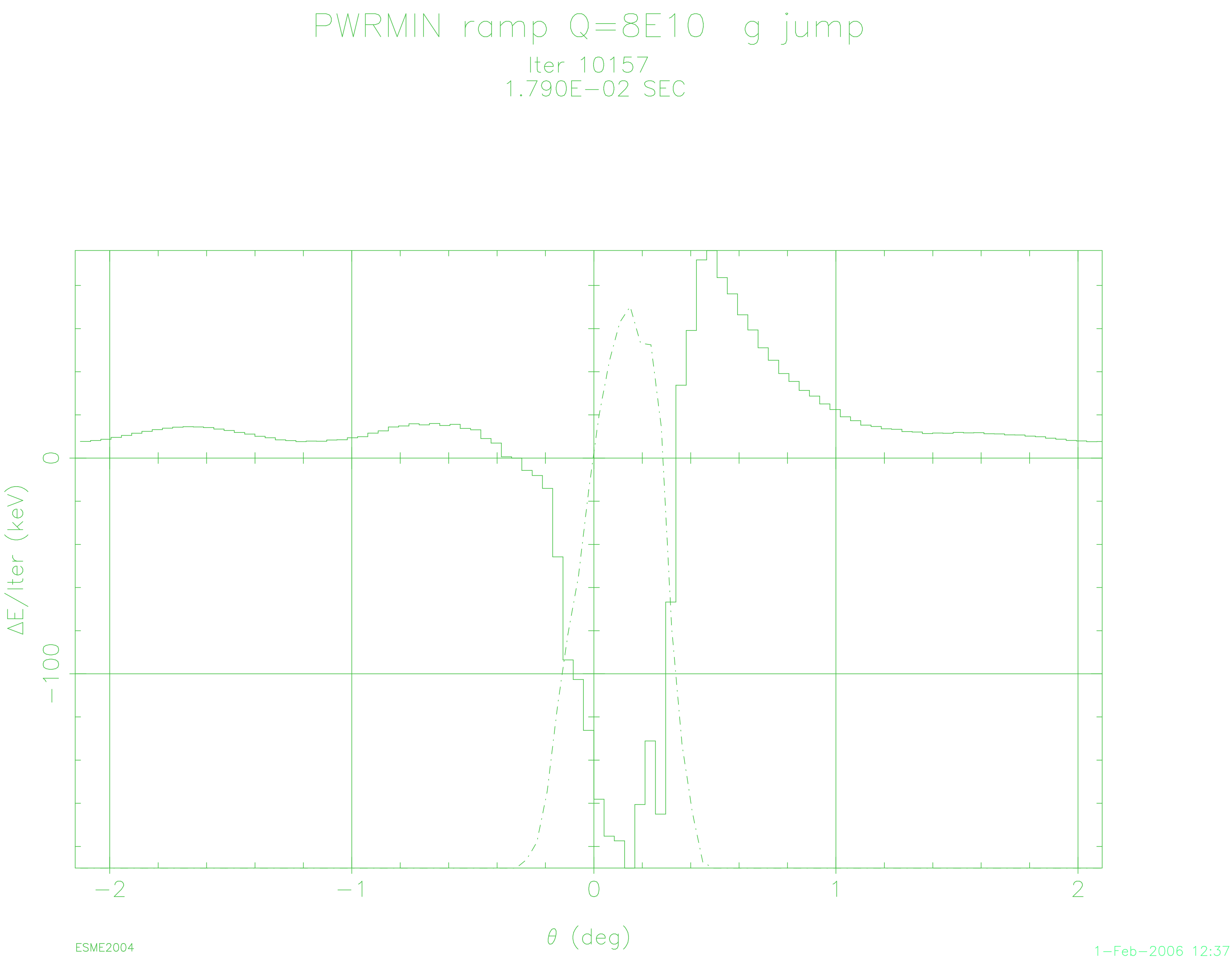

The collective voltage produced by a bunch of $8 \cdot 10^{10}$ protons for the impedance shown in Fig. 3 at transition on the minimax $\dot{B}$ cycle

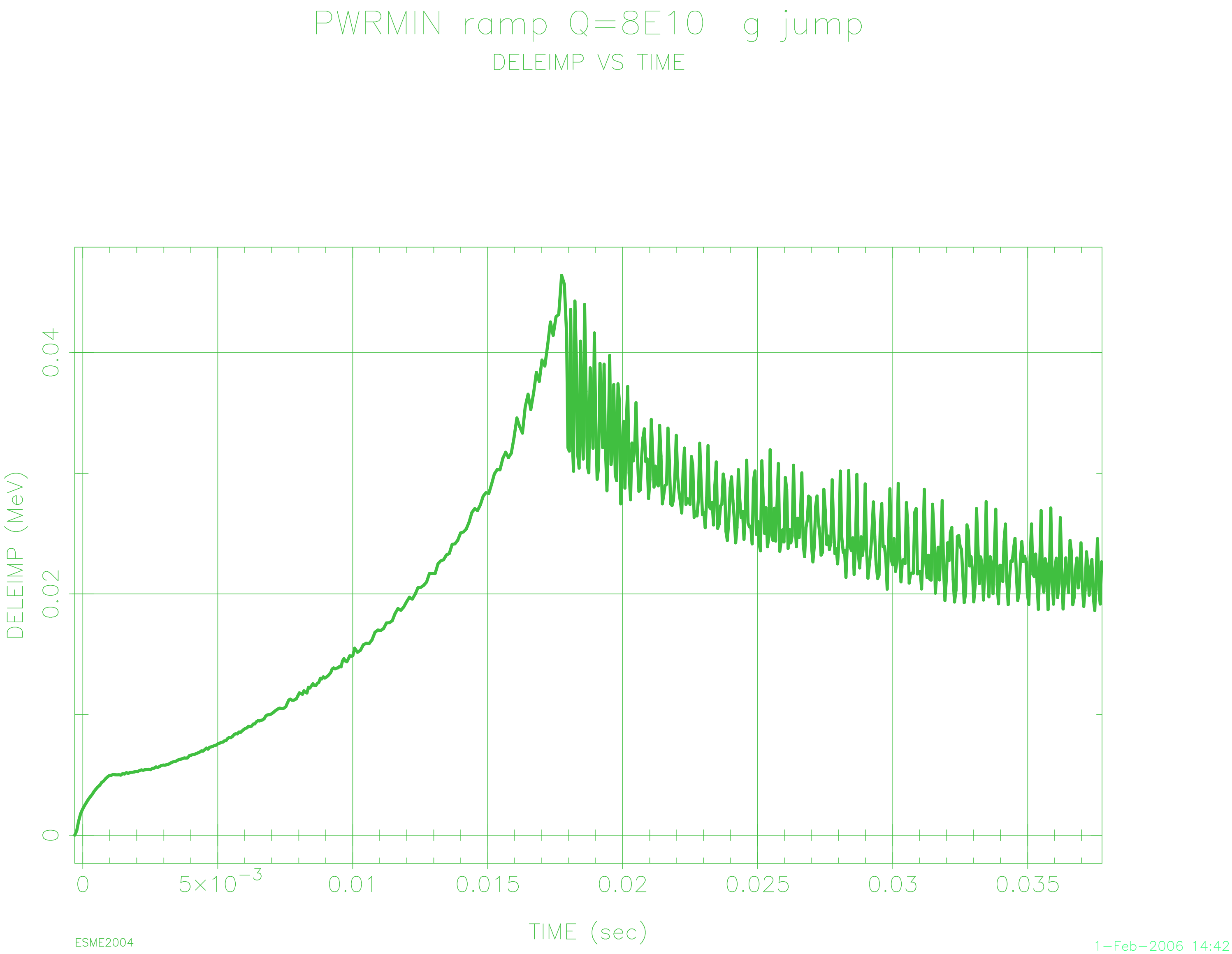

The rf voltage needed to make up the energy loss to the real part of the impedance shown in Fig. 3 during the minimax $\dot{B}$ acceleration cycle with a .3 unit γ_T jump

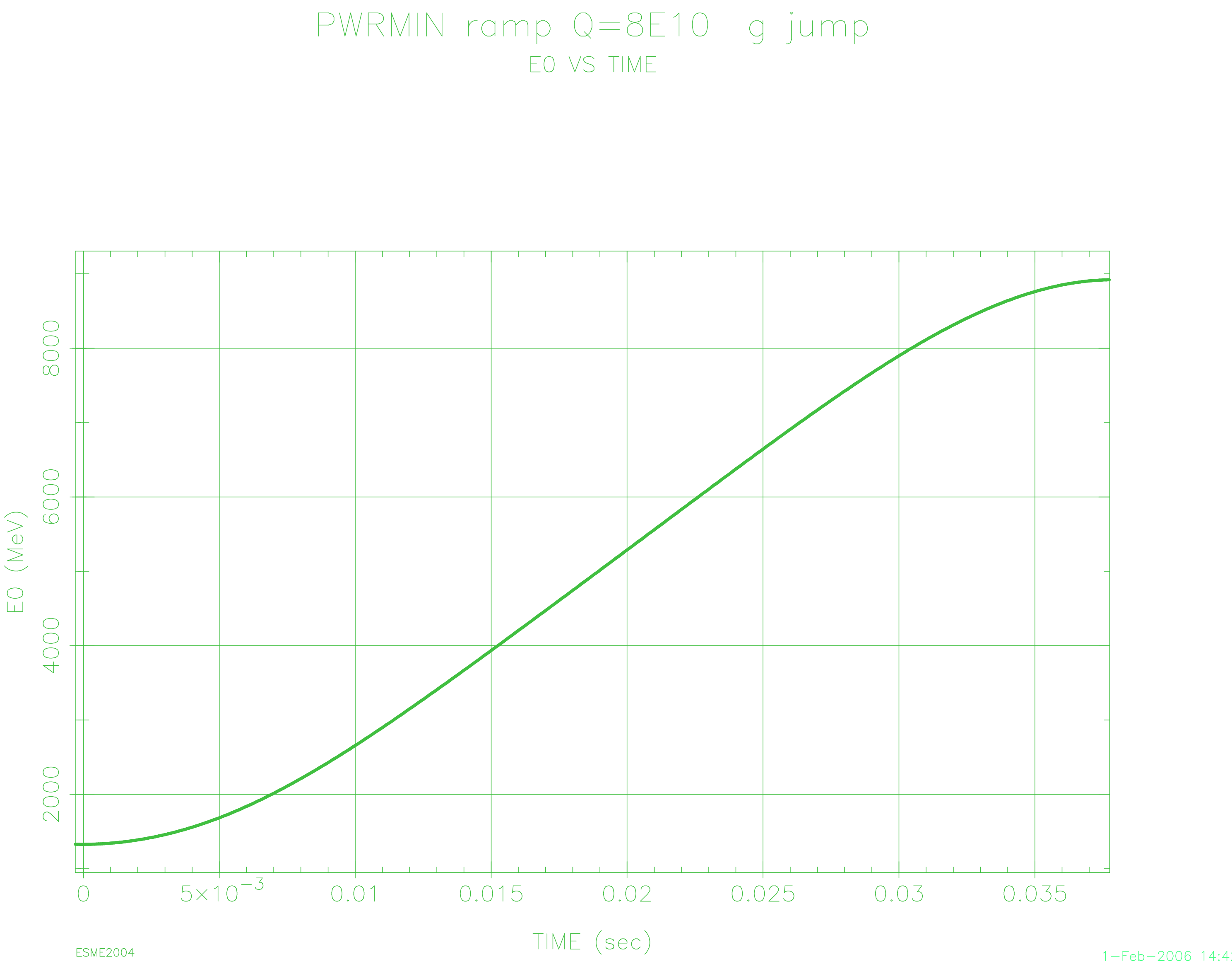

The ramp which minimizes the maximum $\dot{B}$ illustrated by the central orbit energy *vs.* time

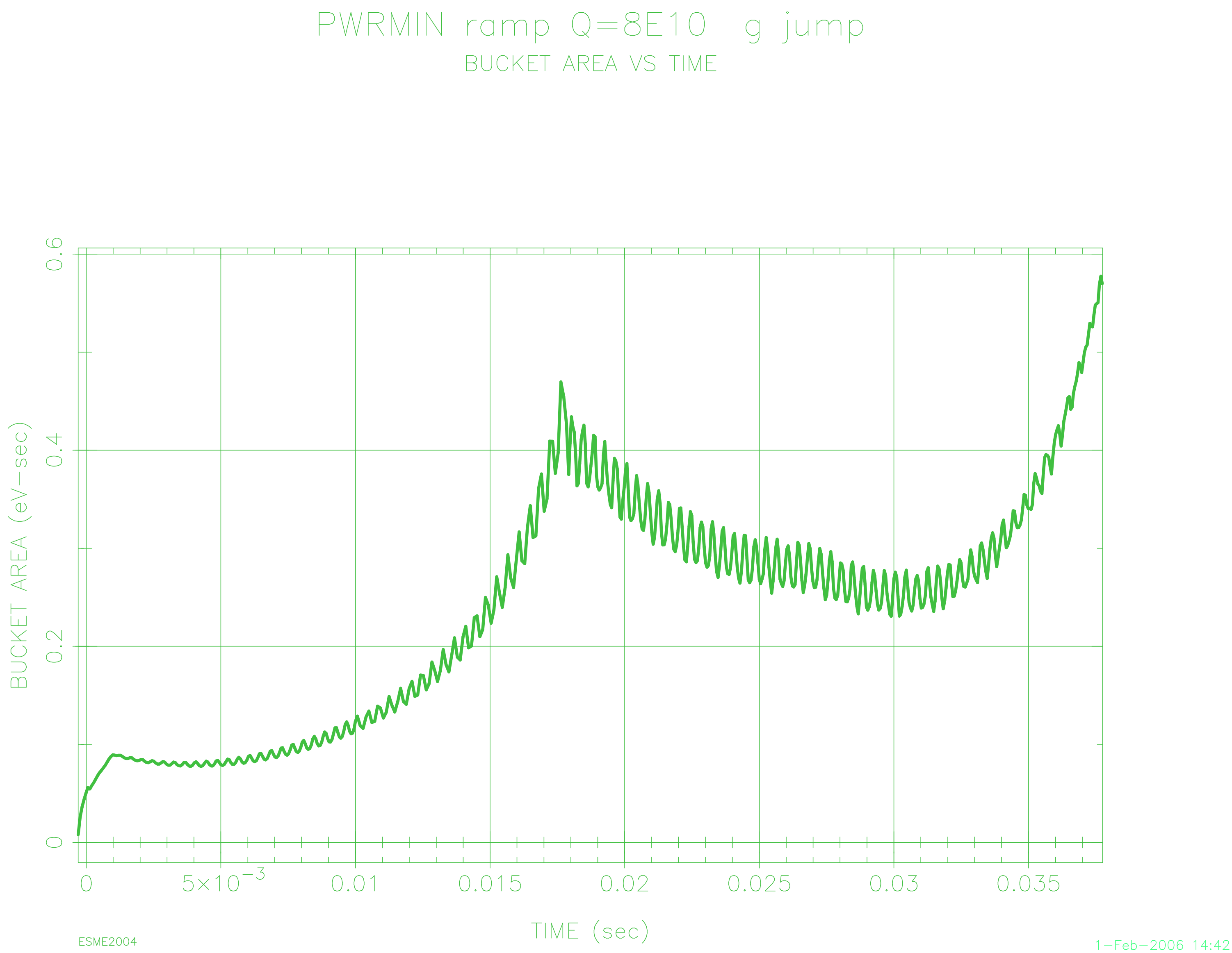

The bucket area [eVs] using the piecewise linear rf voltage curve, the minimax $\dot{B}$ ramp, and a 0.3 unit γ_T jump

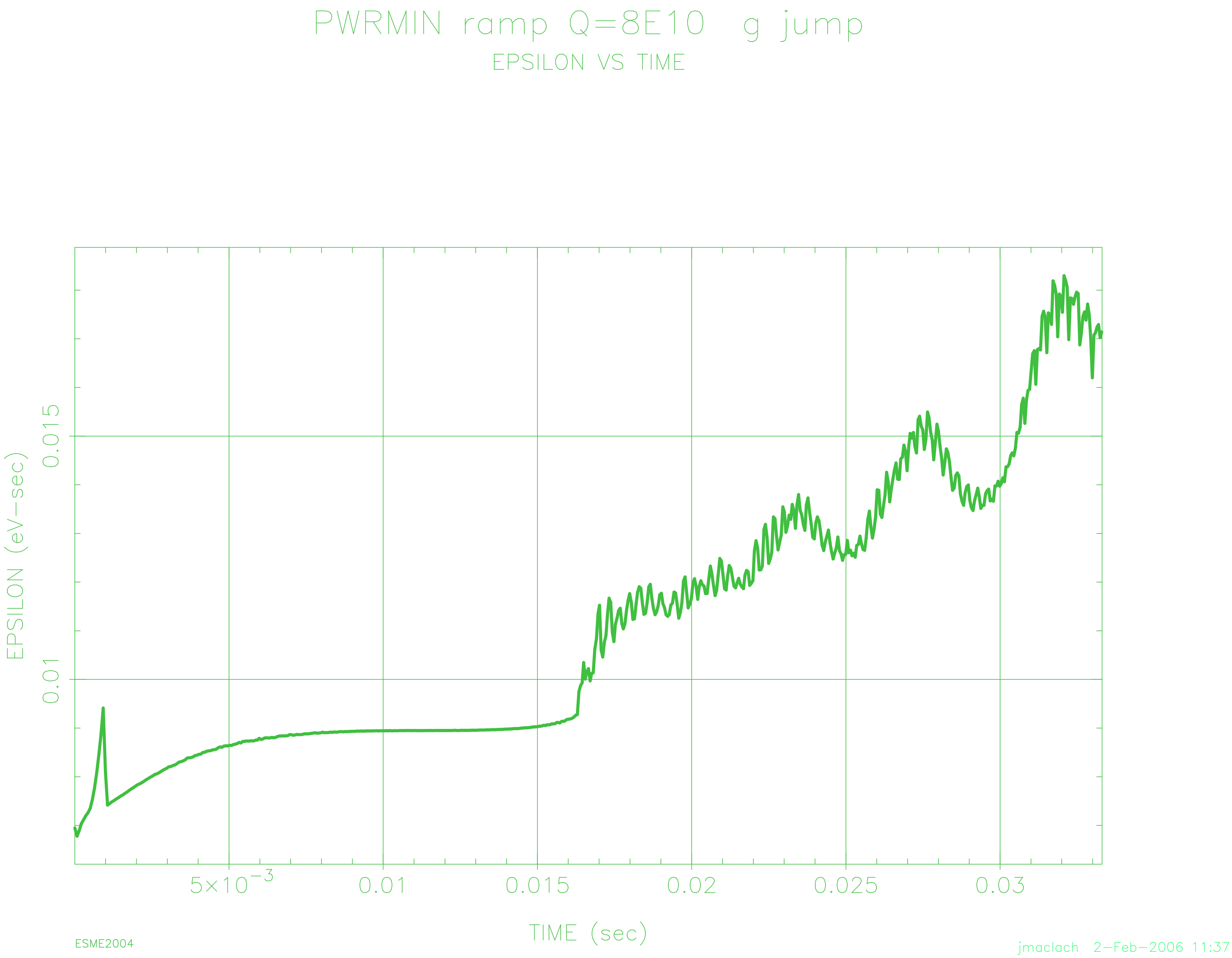

The rms emittance of a bunch of $8 \cdot 10^{10}$ protons captured and accelerated on the minimax $\dot{\mathrm{B}}$ ramp with a 0.3 unit γ_T jump

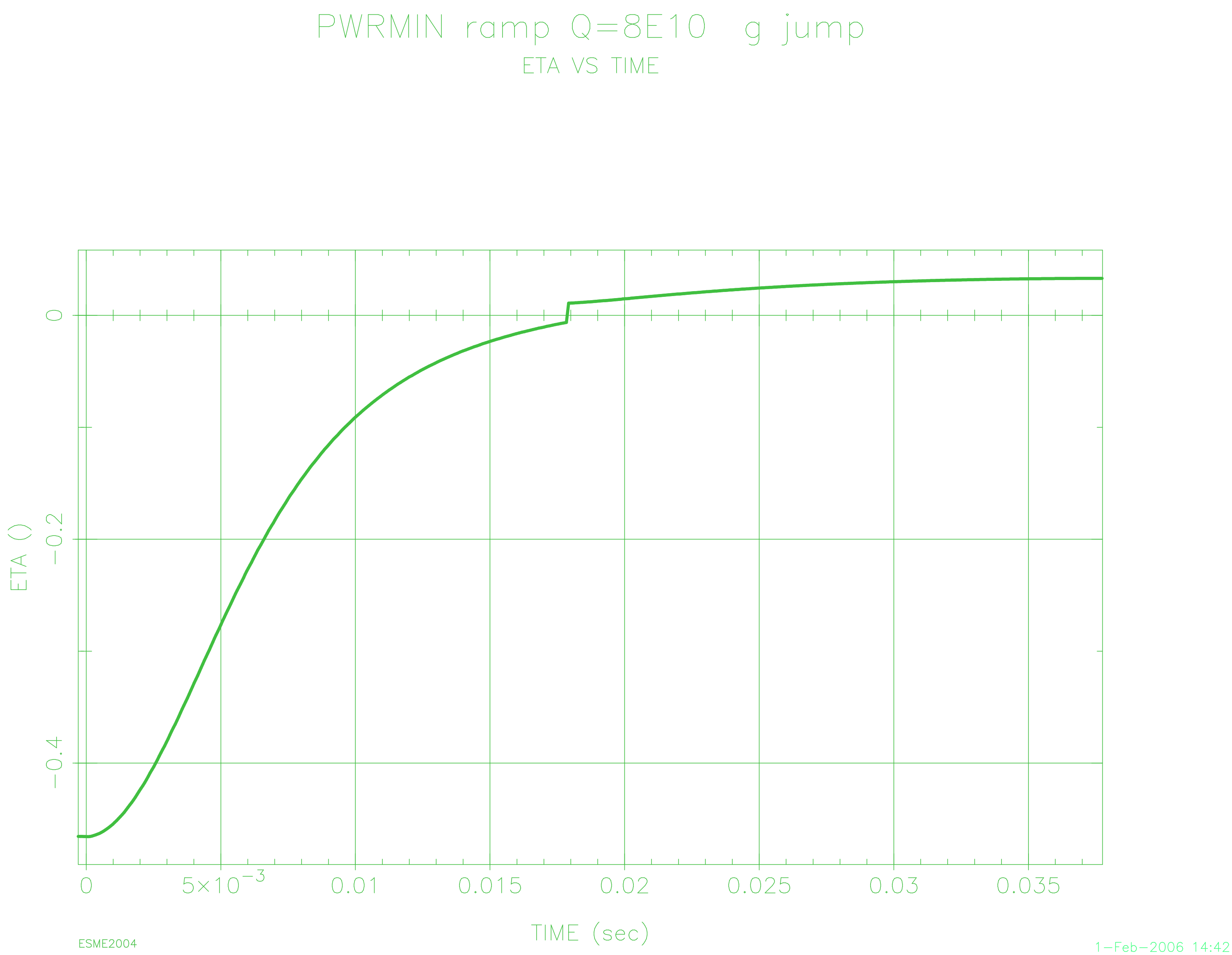

The time slip factor on the minimax $\dot{B}$ ramp with a .3 unit γ_T jump

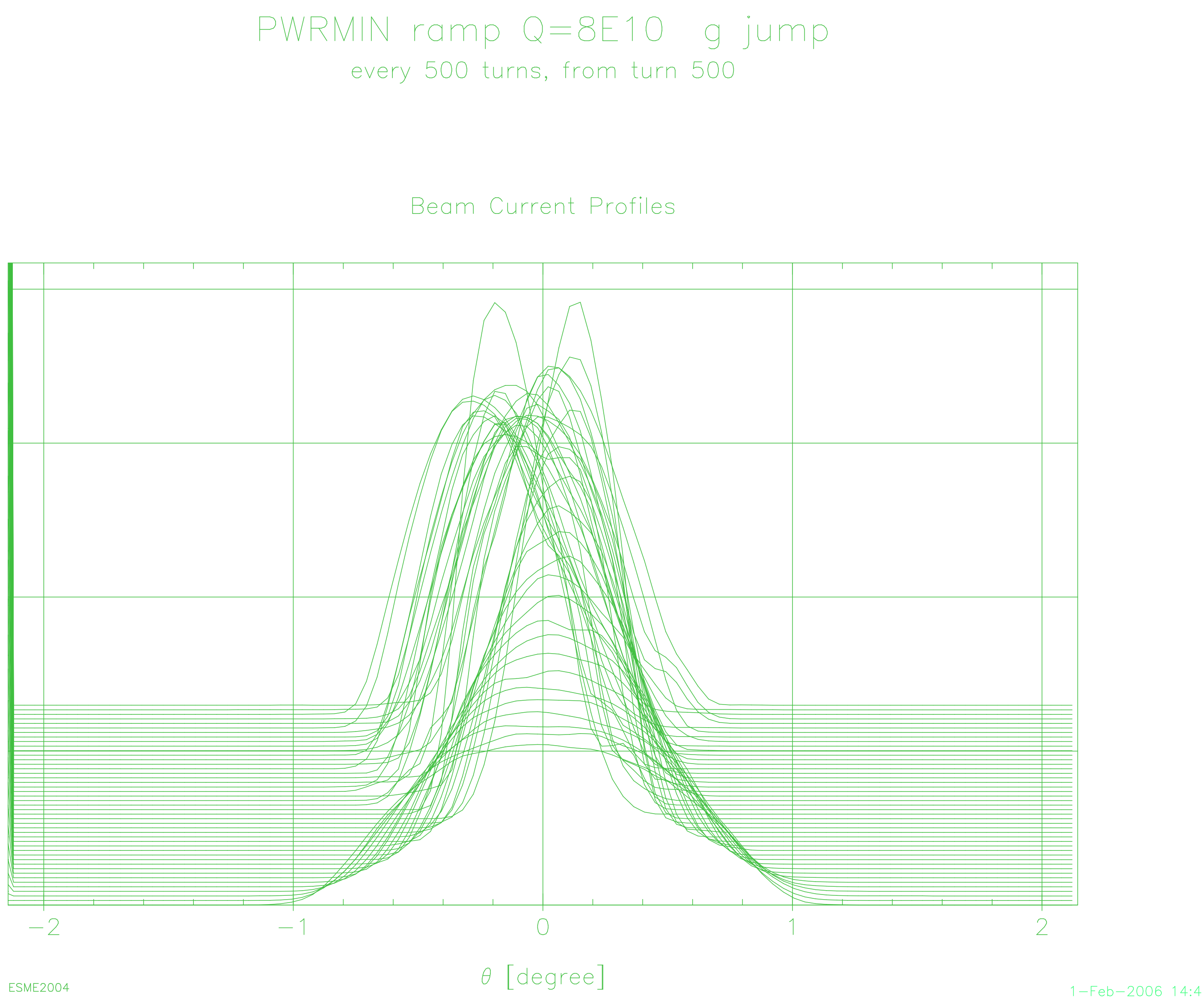

The bunch current at approximately 1 ms (500 turn) intervals for an $8 \cdot 10^{10}$ proton bunch on the minmax $\dot{\mathrm{B}}$ ramp with γ_T jump

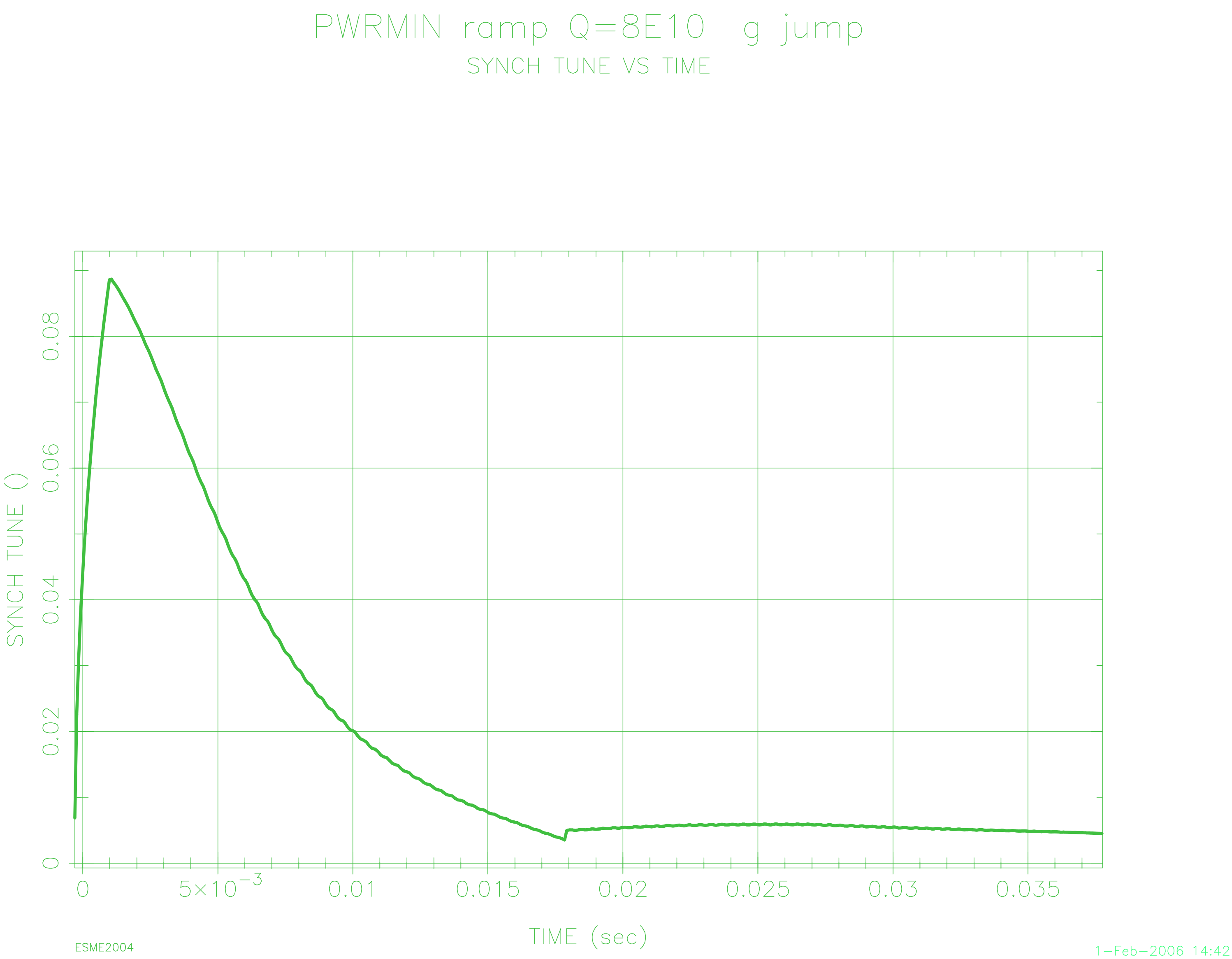

The synchrotron tune on the minimax $\dot{B}$ ramp with γ_T jump

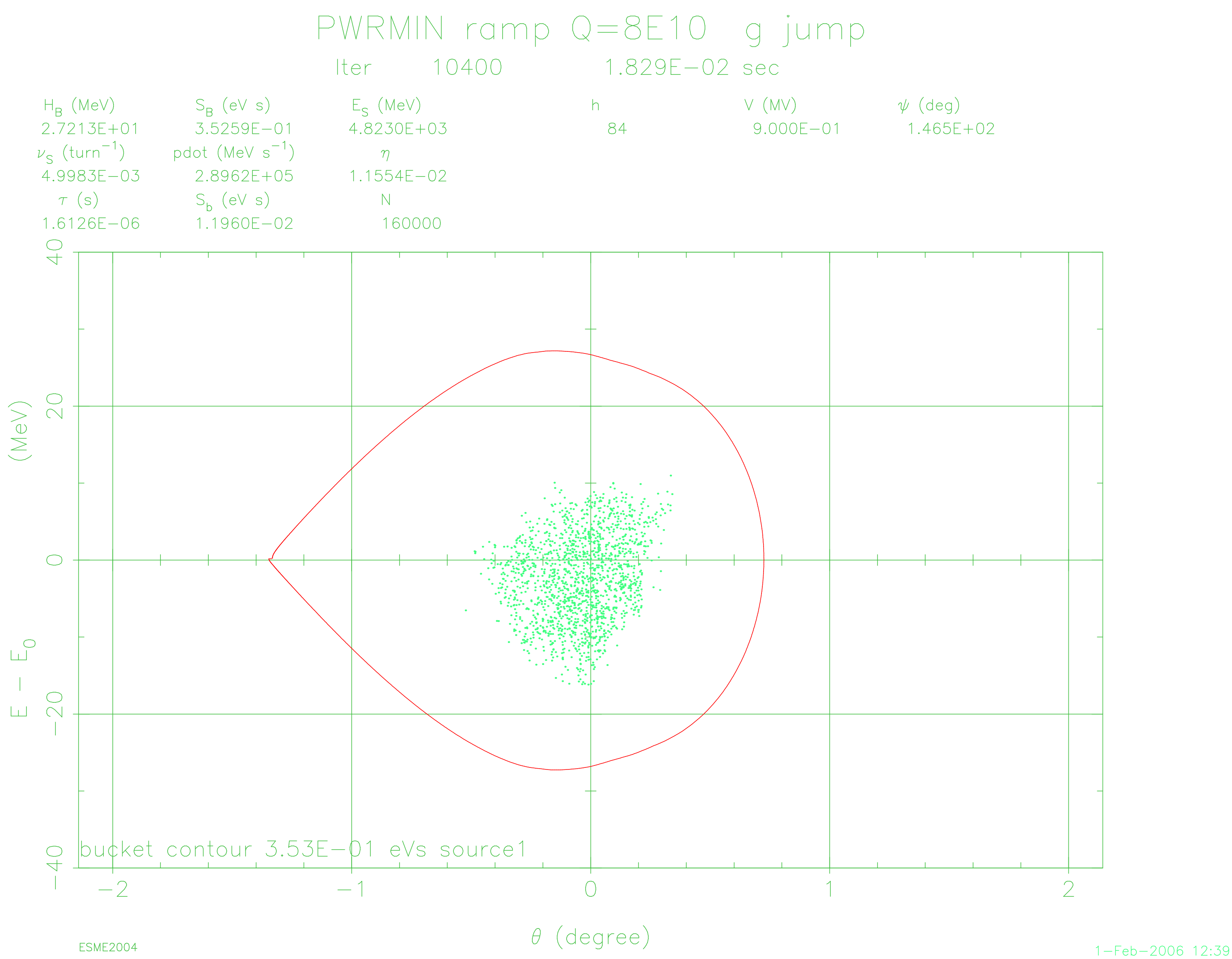

The longitudinal phase space for a bunch of $8 \cdot 10^{10}$ protons just after transition on the minimax $\dot{\text{B}}$ ramp with a 0.3 unit γ_T jump

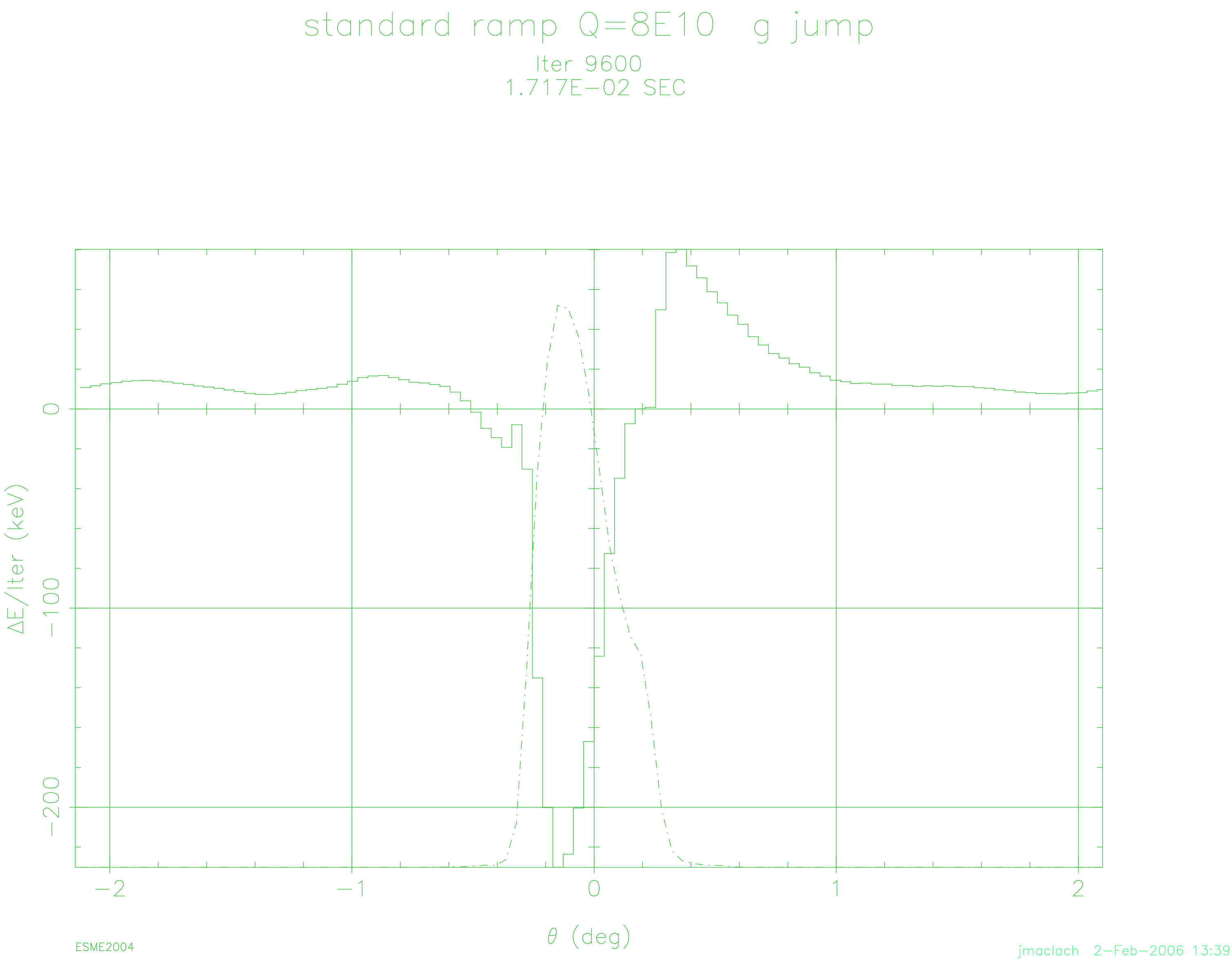

The collective voltage produced by a bunch of $8 \cdot 10^{10}$ protons for the J. Crisp impedance at transition on the standard 15 Hz ramp

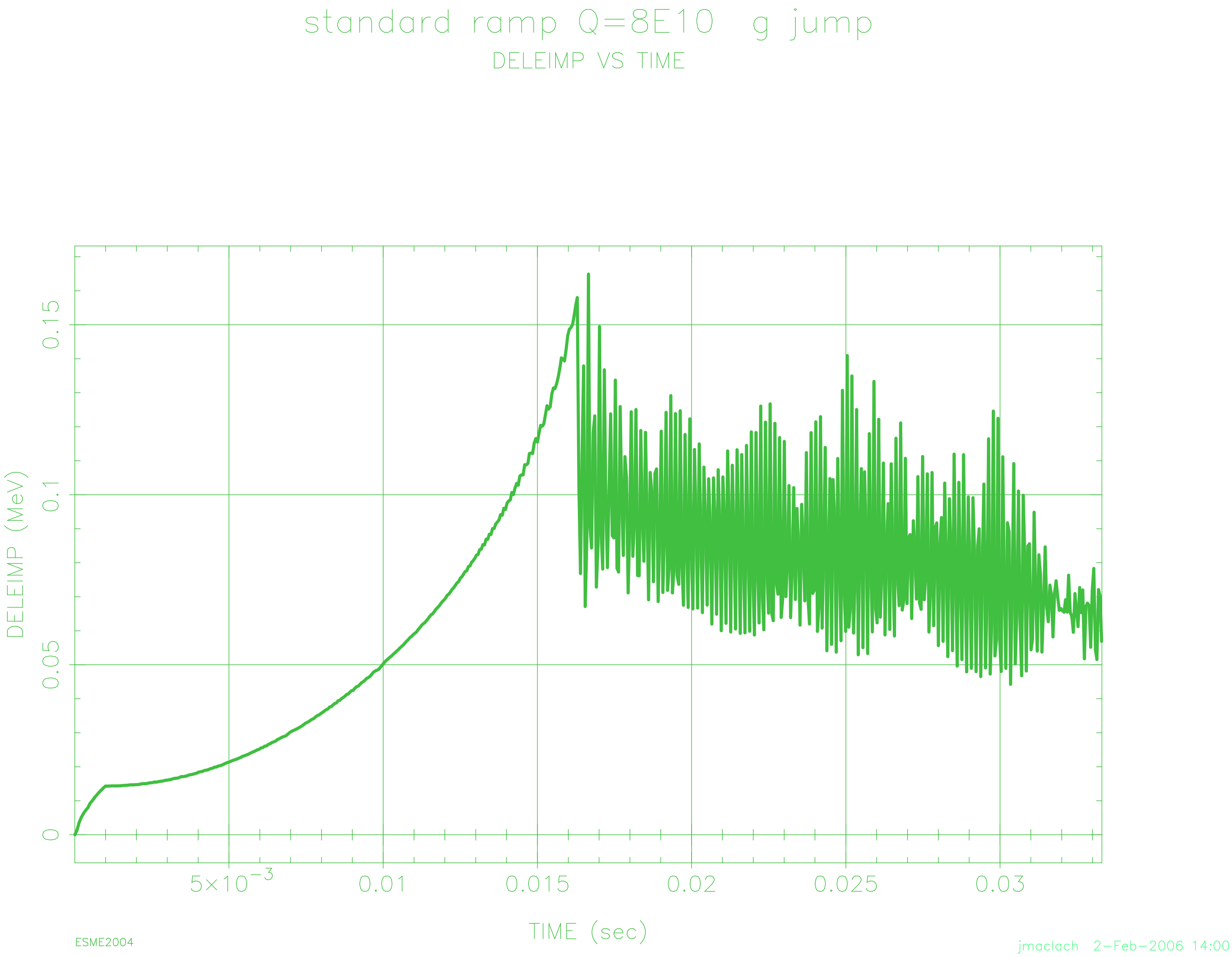

The rf voltage needed to make up the energy loss to the real part of the impedance during the standard 15 Hz cycle with a 0.3 unit γ_T jump

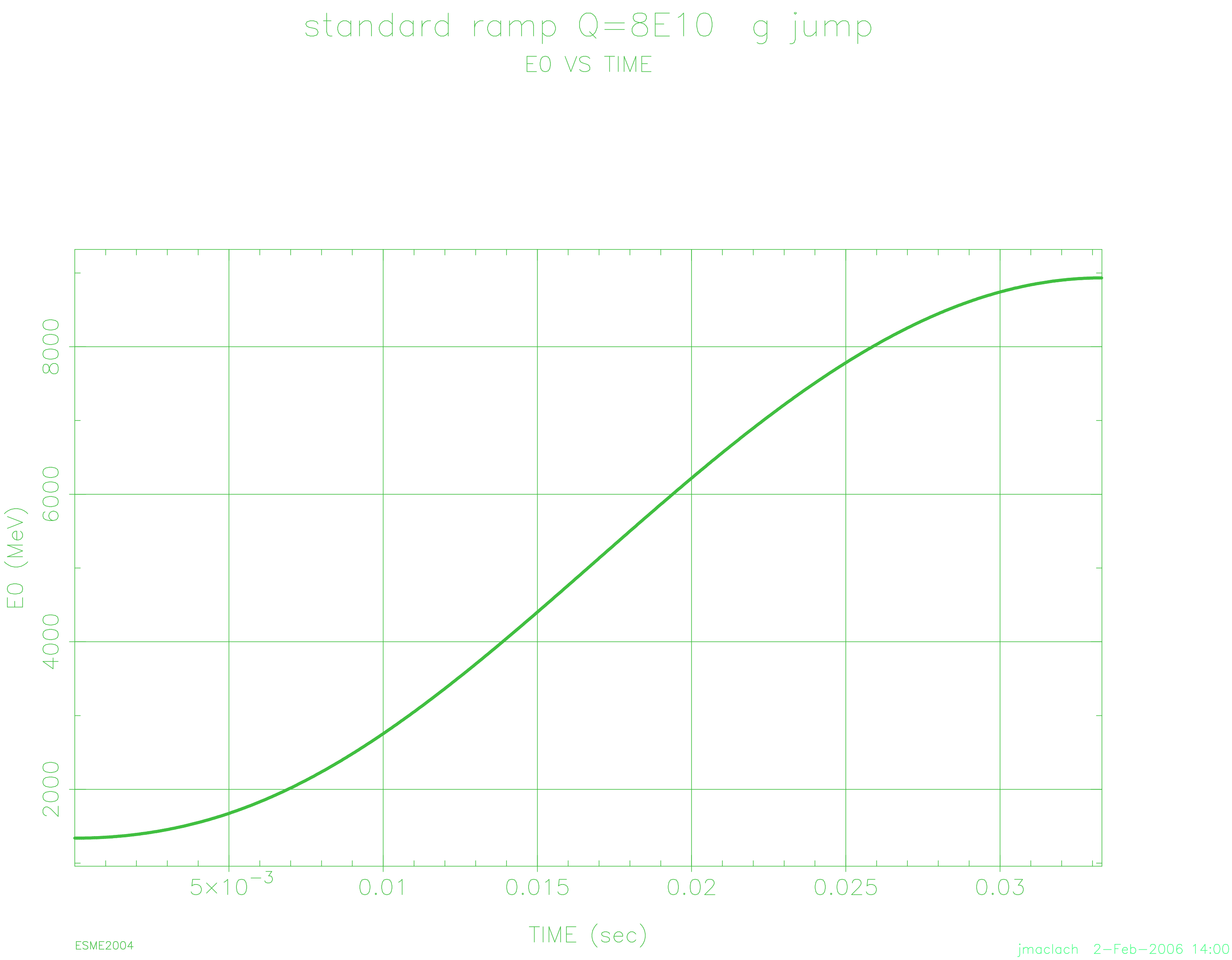

The standard 15 Hz ramp illustrated by the central orbit energy *vs*. time

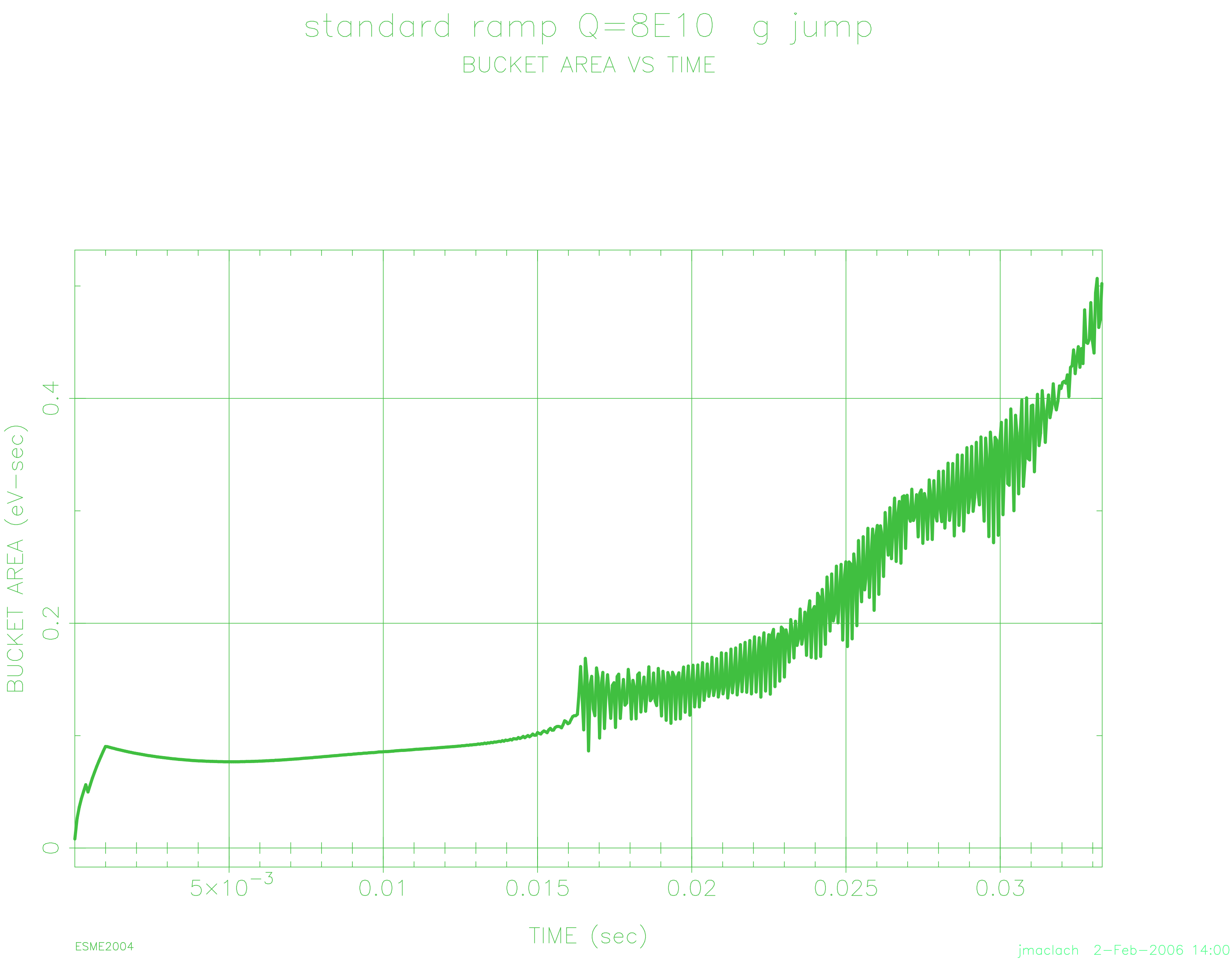

The bucket area [eVs] using the standard 15 Hz ramp, the piecewise linear rf voltage curve, and a 0.3 unit γ_T jump

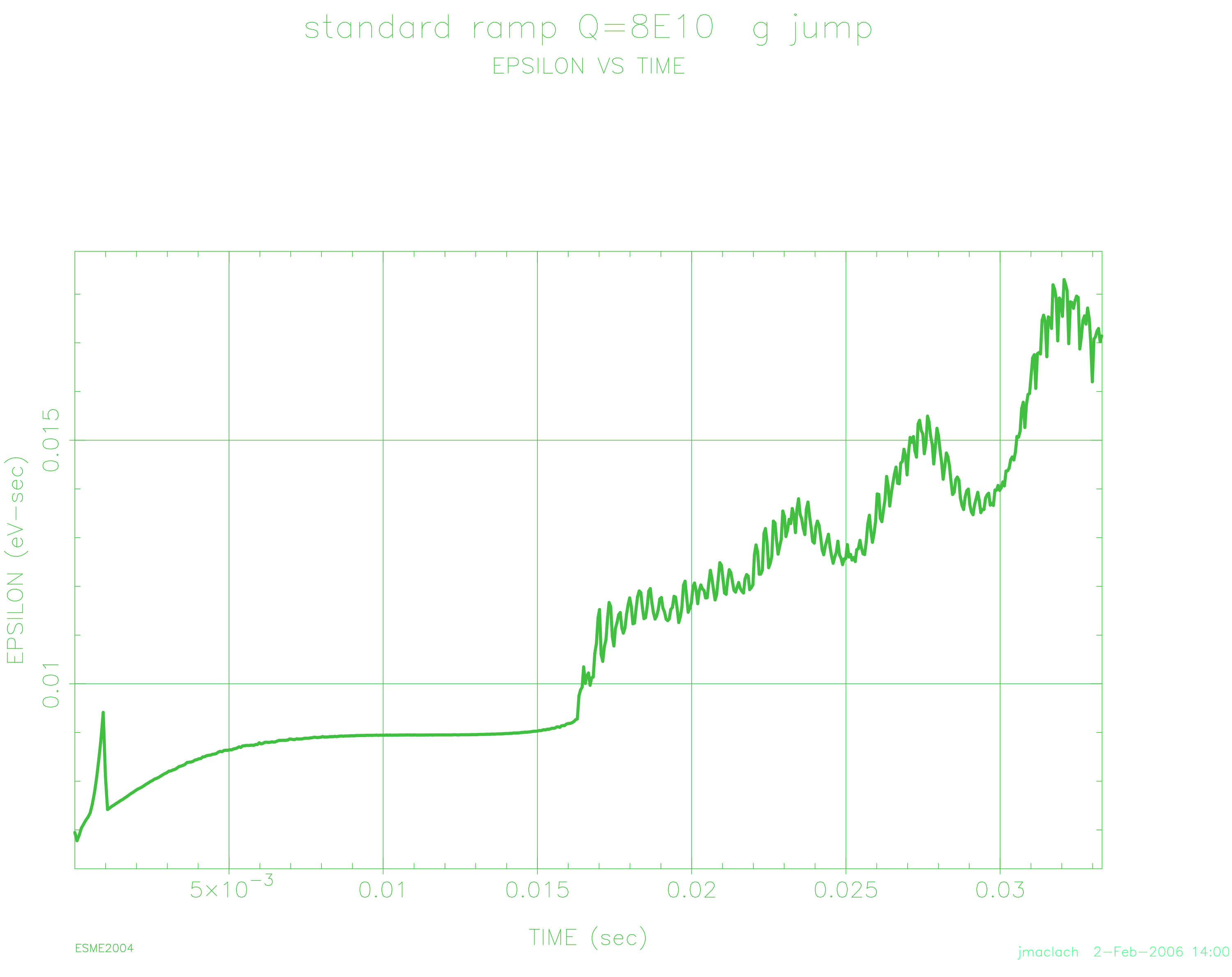

The rms emittance of a bunch of $8 \cdot 10^{10}$ protons captured and accelerated on the standard 15 Hz ramp with a 0.3 unit γ_T jump

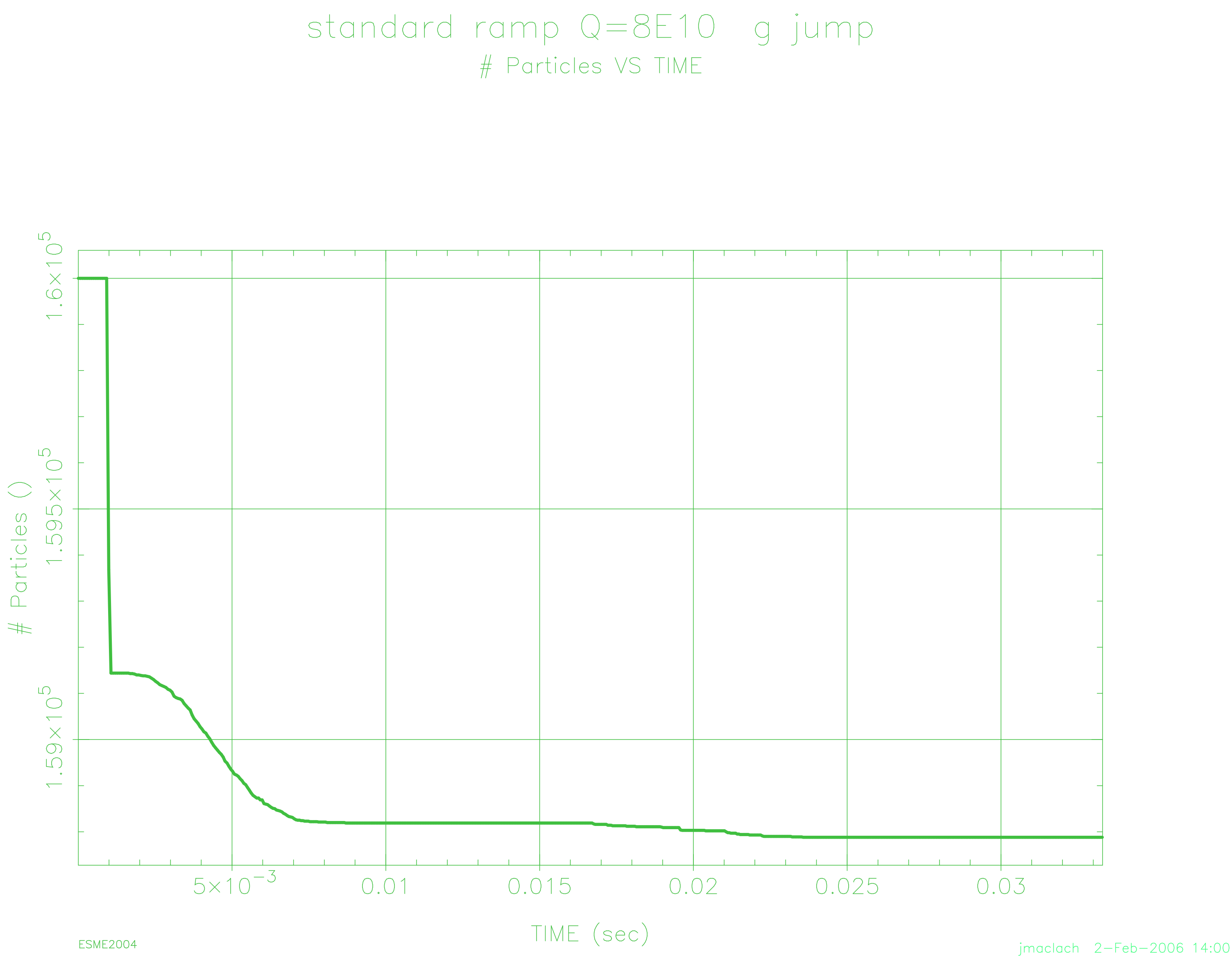

The loss from $1.6 \cdot 10^5$ macroparticles during the standard 15 Hz ramp with a 0.3 unit γ_T jump

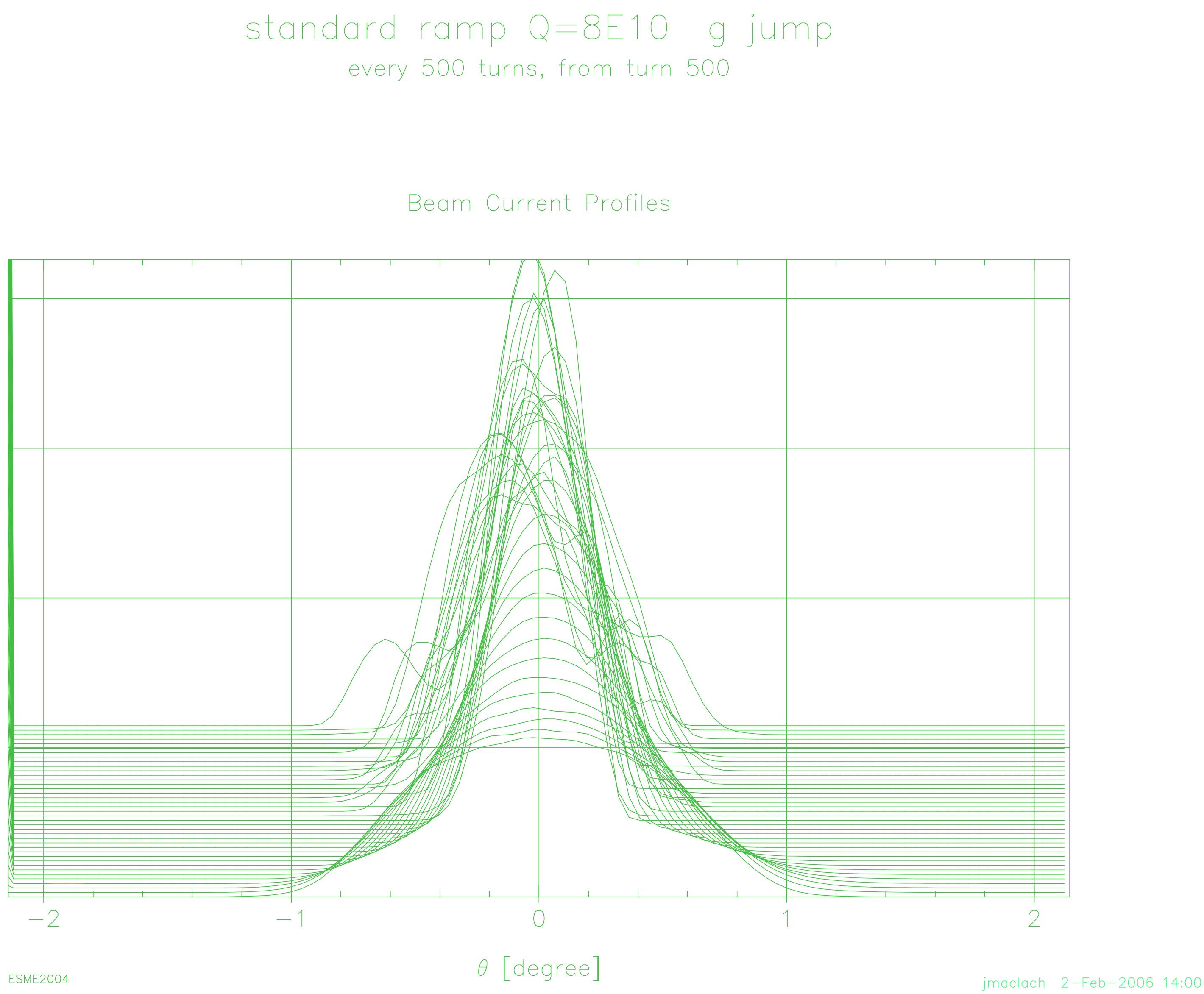

The bunch current at approximately 1 ms (500 turn) intervals for an $8 \cdot 10^{10}$ proton bunch on the standard 15 Hz ramp with γ_T jump

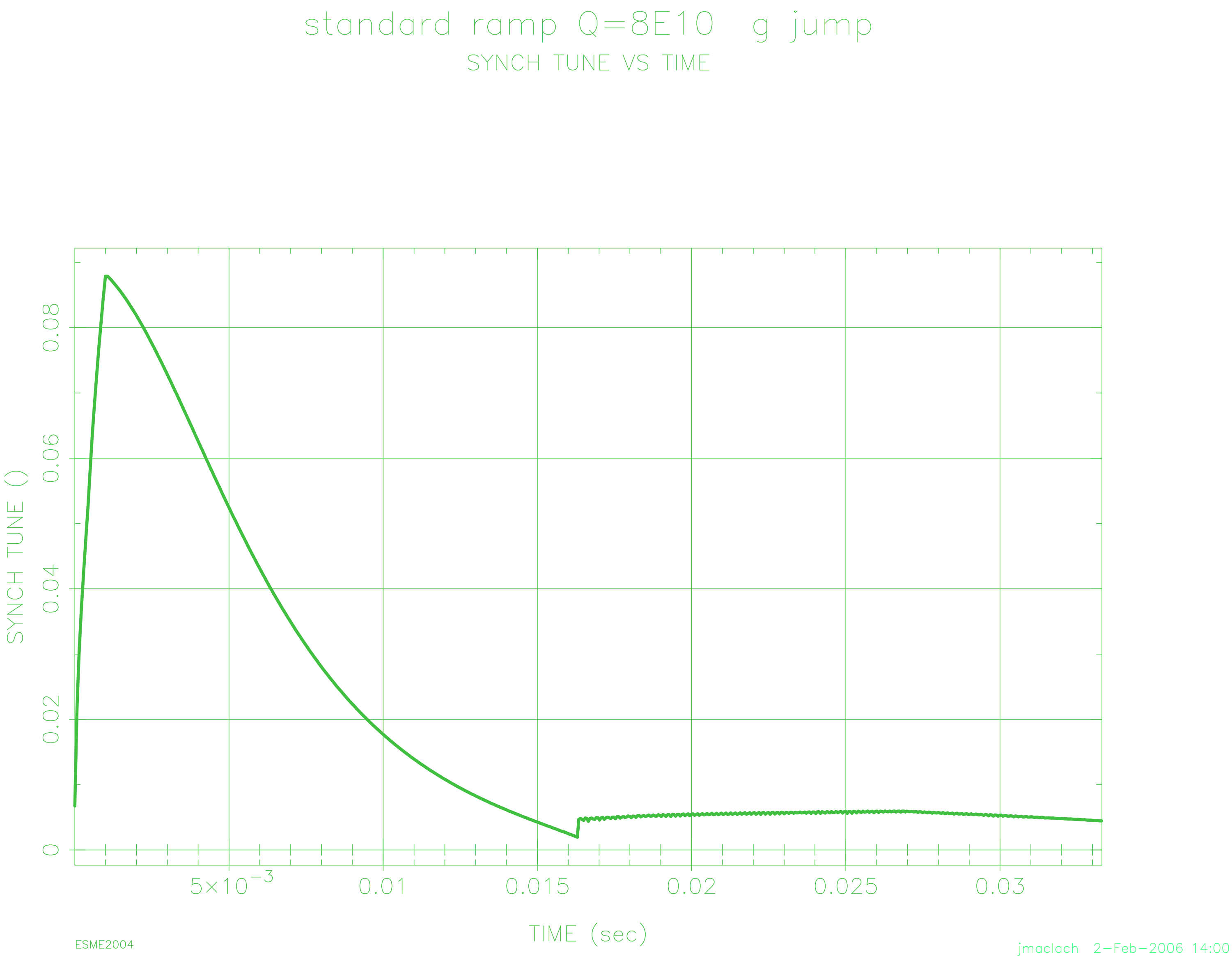

The synchrotron tune ν_s on the standard 15 Hz ramp with a 0.3 unit γ_T jump

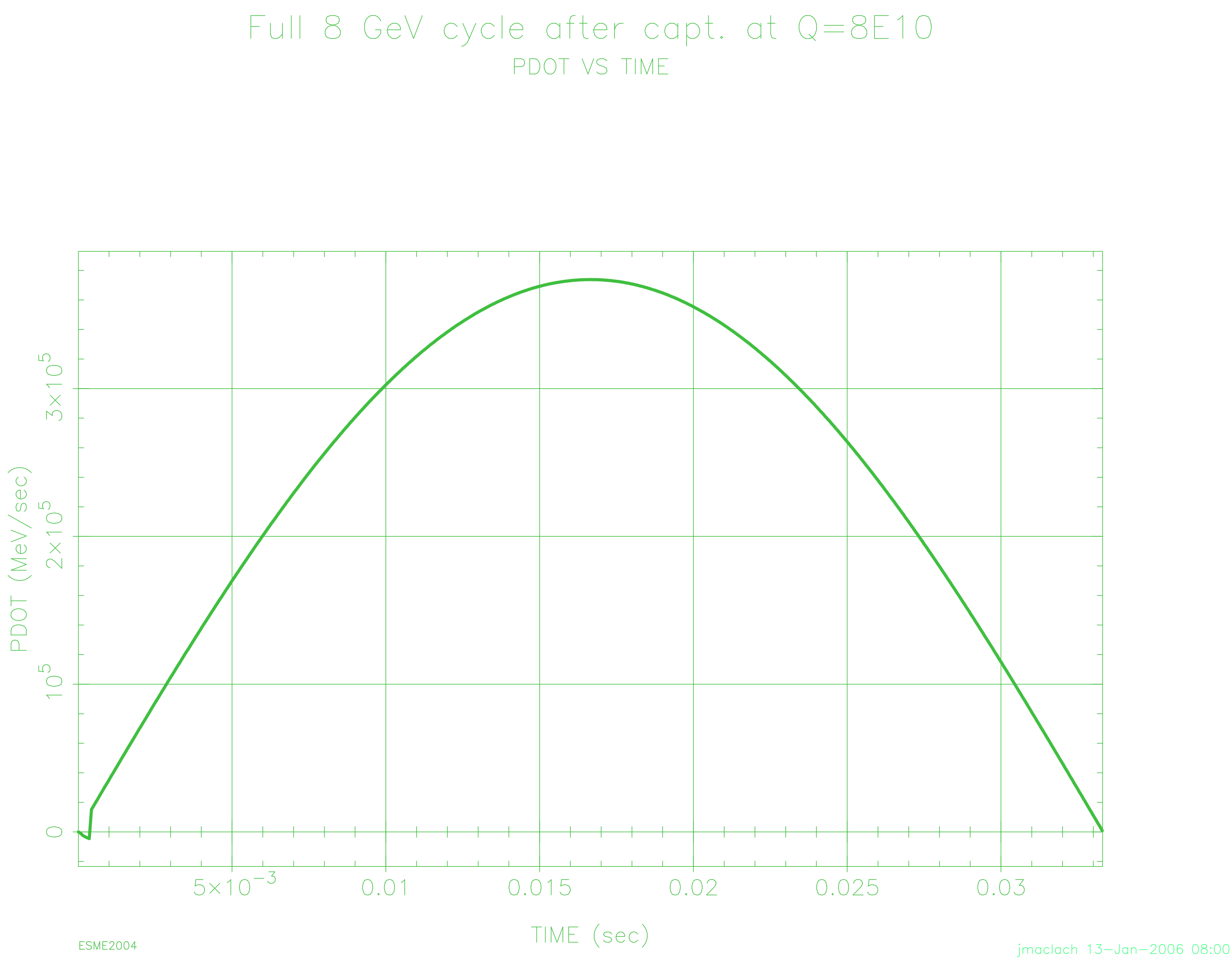

The $\dot{p}$ on the standard 15 Hz ramp with a 0.3 unit γ_T jump

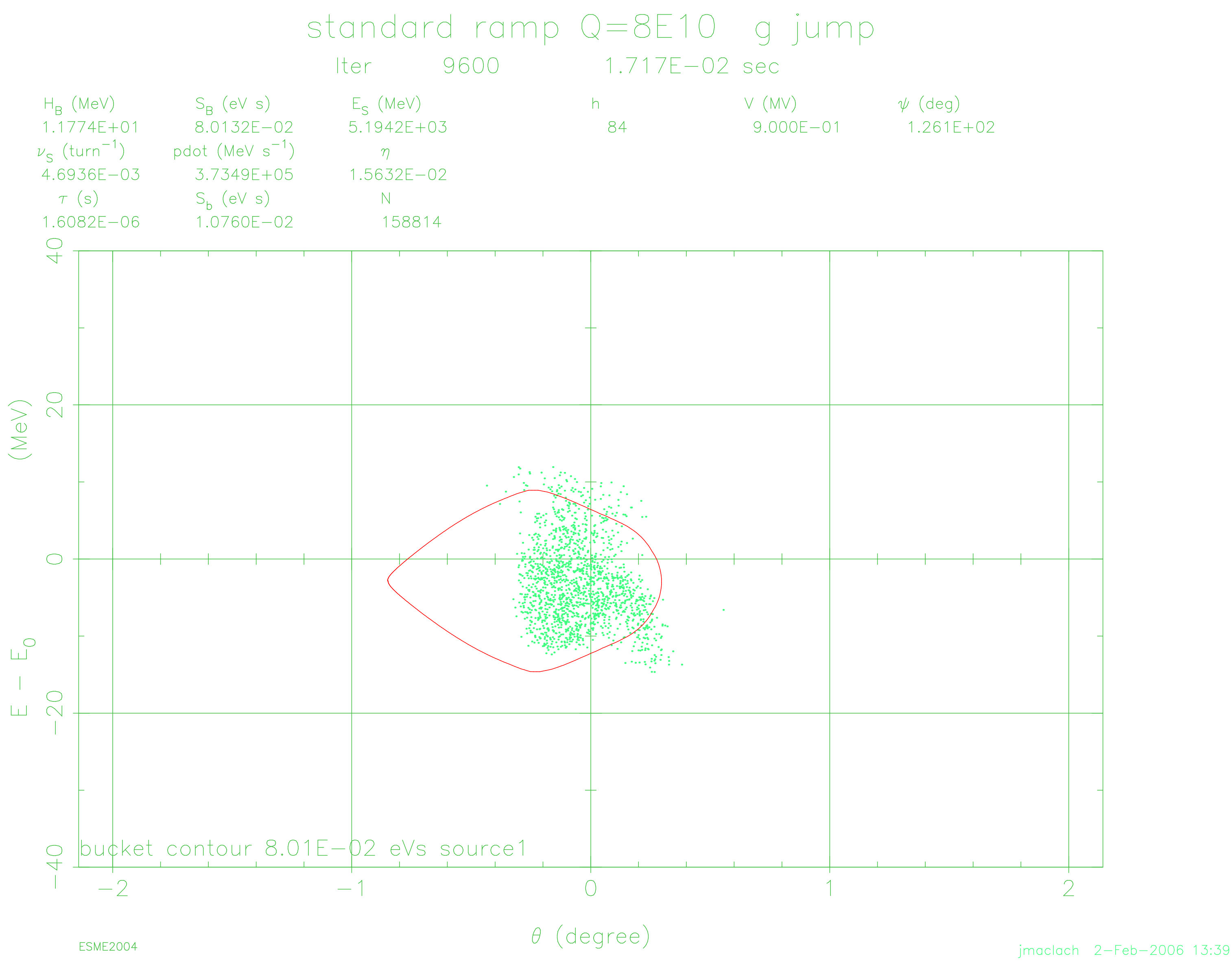

The longitudinal phase space for a bunch of $8 \cdot 10^{10}$ protons just after transition on the standard 15 Hz ramp with a 0.3 unit γ_T jump